

Deep Learning Advances on Different 3D Data Representations: A Survey

Eman Ahmed, Alexandre Saint, Abd El Rahman Shabayek, Kseniya Cherenkova, Rig Das, Gleb Gusev, Djamila Aouada and Björn Ottersten

Abstract—3D data is a valuable asset in the field of computer vision as it provides rich information about the full geometry of sensed objects and scenes. With the recent availability of large 3D datasets and the increase in computational power, it is today possible to consider applying deep learning to learn specific tasks on 3D data such as segmentation, recognition and correspondence. Depending on the considered 3D data representation, different challenges may be foreseen in using existent deep learning architectures. In this paper, we provide a comprehensive overview of various 3D data representations highlighting the difference between Euclidean and non-Euclidean ones. We also discuss how deep learning methods are applied on each representation, analyzing the challenges to overcome.

Index Terms—3D Deep Learning, 3D data representations, Euclidean data, non-Euclidean data.



1 INTRODUCTION

THE rapid increase in the scientific activity on *Deep Learning* (DL) architectures on 2D data has been accompanied and nourished by a notable string of empirical successes in the computer vision field by achieving remarkable results in many tasks such as: classification [1], segmentation [2], [3], [4], detection and localization [5], recognition [6] and scene understanding [7]. The key strength of deep learning architectures are in their ability to progressively learn discriminative hierarchal features of the input data. Most of the DL architectures are already established on 2D data [1]. Established DL architectures on 2D data showed that they require to use a large amount of training data. Due to this fact, applying DL on the 3D domain was not as effective as 2D. Fortunately, with the recent advances in the 3D sensing technologies and the increased availability of affordable 3D data acquisition devices such as structured-light 3D scanners [8] and time-of-flight cameras [9], the amount of the available 3D data has tremendously increased. 3D data provides rich information about the full geometry of 3D objects. Driven by the breakthroughs achieved by DL and the availability of 3D data, the 3D computer vision community has been actively investigating the extension of DL architectures to 3D data.

3D data can have different representations where the structure and the geometric properties vary from one representation to another. In this paper, we study DL techniques employed on different 3D data representations in detail, classifying these representations into Euclidean and Non-Euclidean. 3D Euclidean-structured data has an underlying grid structure that allows for a global parametrization and

having a common system of coordinates. These properties make extending the already-existing 2D DL paradigms to 3D data a straight-forward task, where the convolution operation is kept the same as 2D. 3D Euclidean data is more suitable for analyzing rigid objects where the deformations are minimal [10], [11], [12] such as voxel data for simple objects such as, chairs, planes, etc [13]. On the other hand, 3D non-Euclidean data do not have the gridded array structure where there is no global parametrization. Therefore, extending classical DL techniques to such representations is a challenging task; however, understanding the structure of such representations is important in analyzing non-rigid objects for various tasks such as point-to-point correspondence [14], [15], [16] and segmentation tasks [17] on human body models. In order to expand the scope of DL architectures and ease the applicability of DL models to 3D data, one needs to understand the structural properties of different representations of 3D data, which is the main focus of this paper.

DL on 3D data has become a field in itself, with regular activities in top computer vision scientific venues. Different terminologies are used across different papers. In [18], Bronstein et al. focus specifically on non-Euclidean data and refer to it as *geometric data*. They initiate the term *geometric deep learning* to refer to DL techniques applied on non-Euclidean data. The main purpose of this paper is to extensively study DL advances on all types of 3D data representations. In this paper a comprehensive overview about recent works in the area of DL on different 3D data representations are provided while emphasizing the challenges that are emerging from the structural differences between these data representations. We consider some of the questions that are driving the current research community. Specifically: (i) What is the relationship between the design of DL architecture and the 3D data representation? (ii) What is the optimal set of applications that can be achieved by each representation? Considering the previous questions, we classify the 3D

- E. Ahmed, AER. Shabayek, K. Cherenkova, R. Das, D. Aouada, and B. Ottersten are with the Interdisciplinary center for Security reliability and Trust (SnT), University of Luxembourg, Luxembourg. E-mails: (First name. last name@uni.lu)
- G. Gusev is with Artec Group, Luxembourg.
- K. Cherenkova is with both SnT and Artec Group, Luxembourg.

Manuscript received Month day, year; revised Month day, year.

data representations into Euclidean and non-Euclidean by addressing the properties of both the categories and the formats that fall under each category. A survey presented in [19] is more focused on 3D DL applications in computer vision rather than different data representations. Moreover, authors have covered DL applications on Euclidean data while not considering DL models for non-Euclidean data. Hence, the current work is more comprehensive and it covers the structural aspect of 3D data along with the employed DL models. The contribution of this paper can be summarized as follows:

- A comprehensive survey about the recent advances of DL on various 3D data representations, while distinguishing between the Euclidean and non-Euclidean representations and highlighting the differences between the DL models applied on each category along with the challenges that are imposed to the structure of the data.
- Analysis of the applications and tasks that can be achieved by each data representation are provided using a comparison between different DL techniques for the same task.
- Insights and analysis of the DL models that are employed and an introduction to new research directions.

In order to make this paper self-contained, we start by overviewing various 3D data representations and highlighting the structural differences between Euclidean and non-Euclidean representations, in Section 2. In Section 3, a study on recent advances of DL approaches over the two previously discussed data representations are provided by highlighting the main differences between the network models and the features that are learned by each DL paradigm. Section 4 provides an analysis on the evolution of the use of DL on 3D data and the motivations behind moving from one approach to another by highlighting the limitations of each model and possible areas of improvements.

2 OVERVIEW OF 3D DATA REPRESENTATIONS

The raw 3D data that are captured by different scanning devices come in different forms that vary in both, the structure and the properties. In this section, we go through different representations of 3D data by categorizing them into two main families: Euclidean-structured data and non-Euclidean data. Previous efforts tried to address one or more 3D data representations, but not all of them [25], [26], [27], [28]. The present work is, therefore, more comprehensive and gives an in-depth information about different 3D data representations.

2.1 Euclidean-structured data

Some 3D data representations have an underlying Euclidean-structure where the properties of the grid-structured data are preserved such as having a global parametrization and a common system of coordinates. The main 3D data representations that fall under this category are: descriptors, projections, RGB-D data, volumetric data and multi-view data.

2.1.1 Descriptors

Generally speaking, a shape descriptor is a simplified representation of the 3D object to describe geometric or topological characteristics of the 3D shape. Shape descriptors can be obtained from the object’s surface, texture, depth or any other characteristic or a combination of all [29], [30]. Shape descriptors can be seen as a signature of the 3D shape, which is represented in numeric values to ease processing and computations and allow for comparison among different 3D shapes. The nature and the meaning of this signature depend on the characteristic of the shape descriptor used and its definition. Kazmi et al. [29] and Zhang et al. [30] have published comprehensive surveys about 3D shape descriptors.

3D descriptors provide a compact representation of 3D objects capturing some key properties. Descriptors are usually combined with a learning-based model to extract more hierarchical discriminative features to better represent the shape which will be more elaborately discussed in Section 3.1.1. 3D shape descriptors can be categorized in two different ways; (i) Based on whether the descriptor provides a local or global description of the shape and, (ii) Based on whether the nature of the geometric information captured is intrinsic or extrinsic.

Global descriptors provide a concise yet informative description for the whole 3D shape such as the work presented in [31], [32], [33] while local descriptors provide a more localized representation for smaller patches in the shape like the work presented in [34], [35], [36], [37], [38]. The other categorization is based on the nature of the information described; intrinsic descriptors preserve the intrinsic geometric essence of the features described on the 3D shape such as [38], [38], [39], [40], [41], [42], [43]. Conversely, extrinsic descriptors describe the properties related to a specific realization of the 3D shape in the Euclidean space [34], [36], [44], [45], [46].

2.1.2 3D data projections

Projecting 3D data into another 2D space is another representation for raw 3D data where the projected data encapsulates some of the key properties of the original 3D shape. The type of preserved features is dependent on the projection type itself. Multiple projections have been proposed in the literature where each of them converts the 3D object into a 2D grid with specific features. Projecting 3D data into the spherical and cylindrical domains [47], [48] has been a common practice for representing the 3D data in such format. Such projections help the projected data to be invariant to rotations around the principal axis of the projection and ease the processing of 3D data due to the Euclidean grid structure of the resulting projections as shown in Figure 1, which enables the usage of the well-researched learning models. However, such representations are not optimal for complicated 3D computer vision tasks such as dense correspondence due to the information loss in projection [10].

2.1.3 RGB-D data

Representing 3D data as RGB-D images has become popular in the recent years, due to the popularity of RGB-D sensors

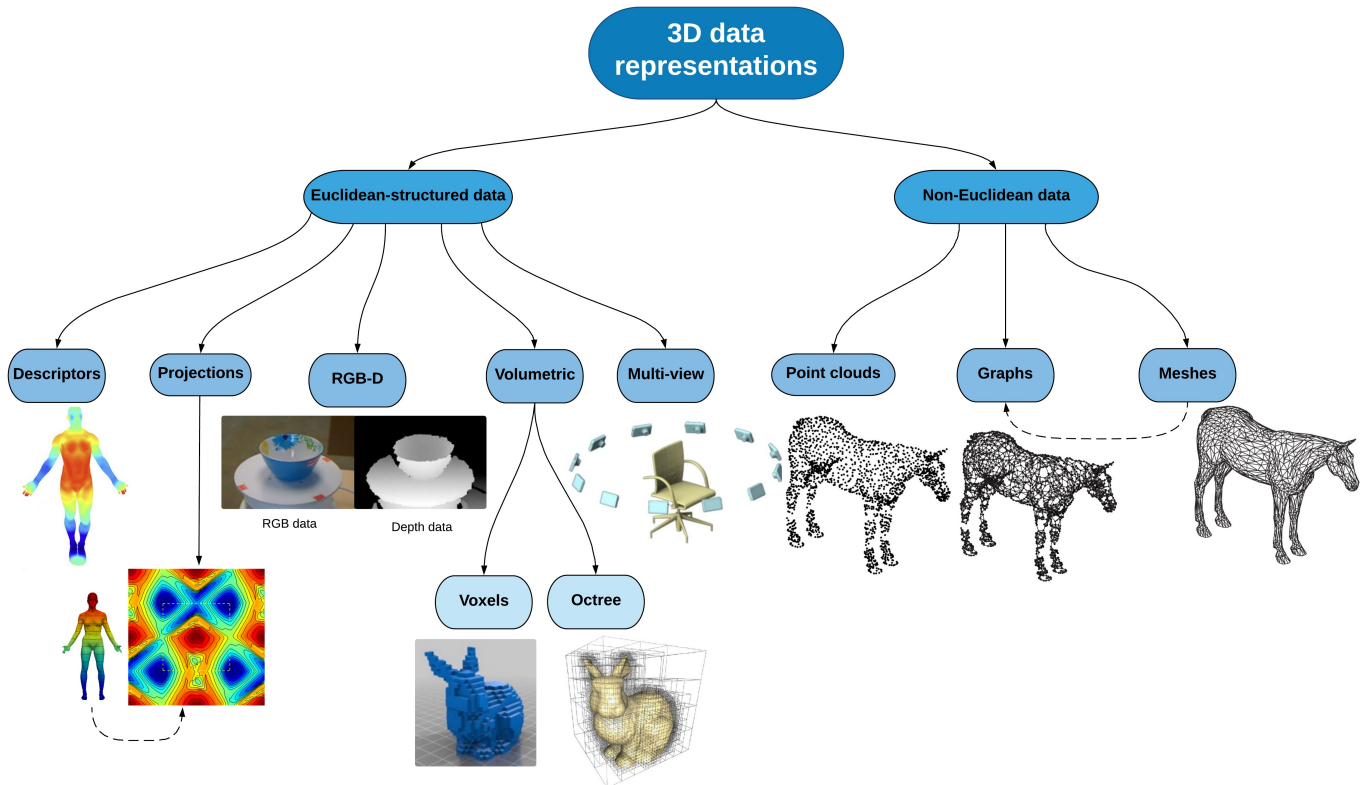


Figure 1: Various representations for 3D data: Euclidean representation (Descriptors [20], Projections [17], RGB-D [21], Volumetric; voxels and octree [22] and multi-view [23]) and Non-Euclidean representations (Point clouds, graphs and meshes) [24].

such as Microsoft’s Kinect [49]. RGB-D data provides a 2,5D information about the captured 3D object by providing the depth map (D) along with 2D color information (RGB) as shown in Figure 1. Besides being inexpensive, RGB-D data are simple yet effective representations for 3D objects to be used for different tasks such as identity recognition [50], pose regression [51] and correspondence [52]. The number of available RGB-D datasets is huge compared to other 3D datasets such as point clouds or 3D meshes [28].

2.1.4 Volumetric data

3D data can be represented as a regular grid in the three-dimensional space. Voxels are used to model 3D data by describing how the 3D object is distributed through the three-dimensions of the scene. Viewpoint information about the 3D shape can be encoded as well by classifying the occupied voxels into visible, occluded or self-occluded. Despite the simplicity of the voxel-based representation and its ability to encode information about the 3D shape, and its viewpoint, it suffers from some constraining limitations [53]. Voxel-based representation is not always efficient because it represents both occupied and non-occupied parts of the scene, which creates a huge unnecessary demand for computer storage. That is why voxel-based representation is not suitable for representing high-resolution data [54], [55].

A more efficient 3D volumetric representation is octree-based [55], which is simply varying-sized voxels. Octree representation models 3D objects as a hierarchical data structure that models occupancy of the 3D object in the 3D

scene [56] as shown in Figure 1. Octree representation is based on recursive decomposition of the root voxels similar to the quadtree structure [54], [57]. The tree divides the 3D scene into cubes that are either inside or outside the object. Despite, the simplicity of forming 3D octrees, they are powerful in representing the fine details of 3D objects compared to voxels with less computations because of their ability to share the same value for large regions of space. However, both voxels and octree representations do not preserve the geometry of 3D objects in terms of the intrinsic properties of the shapes and the smoothness of the surface.

2.1.5 Multi-view data

3D data can be represented as a combination of multi-view 2D images for the same object from different point of views [58] as shown in Figure 1. Representing 3D data in this manner allows learning multiple feature sets to reduce the effect of noise, incompleteness, occlusion and illumination problems on the captured data. Learning 3D data with multi-view 2D data aims to learn a function modelling each view separately and then jointly optimize all the functions to represent the whole 3D shape and to allow generalizing to other 3D shapes. However, the question of how many views are sufficient to model the 3D shape is still open. Representing the 3D object with an insufficiently small number of views might not capture the properties of the whole 3D shape and might cause an over-fitting problem. In addition, too many views cause an unneeded computational overhead. However, learning well-represented multi-view

data proved better performance over learning 3D volumetric data [23].

Both volumetric and multi-view data are more suitable for analyzing rigid data where the deformations are minimal. A good example for such objects is *ModelNet* dataset [13] which is composed of CAD models for primitive objects such as, chairs, tables, desks, etc. Unlike, highly deformable non-rigid objects like the BU4DFE 3D facial expressions dataset [59].

2.2 Non-Euclidean data

The second type of 3D data representations is the non-Euclidean data. This type of data suffers from the absence of the global parametrization and the non-existence of a common system of coordinates or vector space structure [18], which makes processing of such data, quite a challenging task. Considerable efforts were directed towards learning such data and applying DL techniques on it. The main type of non-Euclidean data is point clouds, 3D meshes and graphs. These structures share several common properties that we will discuss throughout this section. It is important to note that both point clouds and meshes can be seen as both Euclidean and non-Euclidean data depending on the scales on which the processing is taking place, i.e., globally or locally. Despite this dual nature, we chose to list them as part of the non-Euclidean data because even if this data looks like Euclidean locally, in practice, they suffer from infinite curvature, self-intersections and different dimensions depending on the scale and location at which one looks [18]. Also, processing such data usually happens on a global scale to learn the whole 3D object’s features which is convenient for complex tasks such as recognition and correspondence.

2.2.1 3D Point clouds

Due to the increased A point cloud can be seen as a set of unstructured 3D points that represent the geometry of 3D objects. Such realization makes it a non-Euclidean geometric data representation. However, point clouds can also be realized as a set of small Euclidean subsets that have a global parametrization and a common system of coordinates and invariant to transformations such as translation and rotation. That is why the definition of the point cloud’s structure depends on whether one is considering the global or the local structure of the object. Since, most of the learning techniques strive for capturing the whole features of the object to perform complex tasks such as recognition, correspondence, matching or retrieval; we classified point clouds as non-Euclidean data.

Despite the ease of capturing point clouds using any of the available technologies such as Kinect [49] and structured light scanners [60], processing them is a challenging task due to some problems related to their data-structure and to capturing them from the environment. The data-structure related problems usually emerge due to the lack of connectivity information in the point clouds, which makes the surface information ambiguous. Furthermore, the environment-related problems are usually present in the real acquisition setup, the raw captured point clouds suffer from noise, incompleteness, irregular sampling density and sometimes holes and missing parts. This happens due to different reasons such as limitations of the sensors [61], some

physical factors or artifacts in the scene [62]. Motivated by the use of point clouds in multiple computer vision tasks e.g. 3D reconstruction [63], object recognition [64] and vehicle detection [65], a lot of work has been done on processing point clouds for noise reduction such as the work done in [66] with a purpose of filtering 3D point clouds from noise while preserving geometric features.

2.2.2 3D meshes and graphs

3D meshes are one of the most popular representations for 3D shapes. A 3D mesh structure consists of a set of polygons called faces described in terms of a set of vertices that describe how the mesh coordinates exist in the 3D space. These vertices are associated with a connectivity list which describes how these vertices are connected to each other. The local geometry of the meshes can be realized as a subset of a Euclidean space following the grid-structured data. However, on a global aspect, meshes are non-Euclidean data where the familiar properties of the Euclidean space are not well defined such as shift-invariance, operations of the vector space and the global parametrization system.

Learning 3D meshes is a challenging task because of two main reasons: DL methods haven’t been readily extended to such irregular representations besides such data usually suffer from noise, missing data and resolution problems such as [67]. 3D meshes can also be presented as graph-structured data where the nodes of the graph correspond to the vertices of the mesh and the edges represent the connectivity between these vertices. Graphs can be directed or undirected. As discussed in Section 3.2, recent work has been done for exploiting such data to learn the properties of 3D objects. Analyzing the spectral properties of the graphs enabled researchers to use the eigen-decomposition of the graph Laplacian to define a convolution-like operation on graphs or meshes converted to graphs [15]. Such a start opened the door for promising innovations in processing geometric data.

3 DEEP LEARNING ARCHITECTURES ON DIFFERENT 3D DATA REPRESENTATIONS

Deep Learning has led to a remarkable impact on the field of computer vision achieving state-of-art results on several 2D computer vision tasks [1], [2], [3], [4], [5], [6], [7], DL started gaining popularity in the 3D domain attempting to make use of the rich 3D data available while considering its challenging properties. However, extending DL models to the 3D domain is not straightforward due to the complex geometric nature of 3D objects and the large structural variations emerging from having different 3D representations.

Having different 3D data representations has led researchers to pursue different DL routes to adapt the learning process to the data properties. In this section, we overview different DL paradigms applied on 3D data classifying these approaches into two different families based on the data representation: DL architectures on Euclidean-structured data and DL architectures on non-Euclidean data with an abstract illustration of the used methods are depicted in Figure 2.

3.1 Deep learning architectures on 3D Euclidean-structured data

The first type of 3D DL approaches is the Euclidean approaches which operate on data with an underlying Euclidean-structure. Due to the grid-like nature of such data, the already established 2D DL approaches can be directly applied. Representing 3D data in a 2D way implies that the initial 3D representation is subjected to some processing to produce a simpler 2D representation on which the classical 2D DL techniques can operate. This processing evolved over years resulting in different 2D representations for 3D data with different properties and characteristics. DL architectures are adapted to each representation trying to capture the geometric properties of this data representation.

Initially, researchers made use of the already established developments in the feature extraction algorithms [68], [69] to extract features from 3D data. This produced grid-like shallow features where 2D DL models can be directly applied. However, considering the complexity of 3D data, this type of methods does not discriminatively learn the intrinsic geometric properties of the shape and needs an exhaustive fine-tuning process. This pushed towards exploiting the depth modality directly from the RGB-D data with DL models. Despite being effective in some applications, this type of data is not suitable for analyzing complex situations due to the noise and the artifacts from acquisition devices [28]. This motivated researchers to apply DL approaches on 3D data directly such as volumetric data and multi-view data. In this section, we cover different DL architectures based on the aforementioned data representations discussing the main strengths and weaknesses of each model and the type of features learnt in each case.

3.1.1 Deep learning architectures on 3D data descriptors

Low-level descriptors have been used as a significant part of the learning process for 3D data. Although multiple handcrafted low-level descriptors were proposed in the literature [68], [69], they suffer from several significant limitations, as they cannot learn the discriminative features from 3D shapes. Hence, the global and local structure the 3D shapes cannot be preserved. Fortunately, DL models are effective in learning hierarchical discriminative features that can generalize well to other unseen data. That is why low-level descriptors have been combined with DL architectures to learn more informative high-level features of the 3D object as shown in the descriptors processing pipeline in Figure 2. This common practice was followed by Liu et al. [70] to learn high-level features for classification and retrieval tasks. Low-level features are encoded in the visual Bag-of-Words (BoW) representation, which then are fed to the Deep Belief Networks (DBNs) to learn high-level semantic features. Experiments on 3D classification and retrieval tasks showed that the learnt features are discriminative against inter-class variations achieving better results than the classical BoW low-level features. In [71] Bu et al. proposed a three-stage pipeline to learn the geometric properties of 3D shapes. Their main idea was to use low-level features extracted to build middle-level position-independent geometric features on which a DL model can be employed to learn the hierarchical high-level features of the 3D shape.

In this method, both Scale-Invariant Heat Kernel Signature (SI-HKS) [38] and Average-Geodesic Distance (AGD) were employed as local low-level descriptors. Then, the Spatially Sensitive Bag-of-Words (SS-BoW) was employed to capture the relationship between spatially close words composed of the extracted low-level features. Finally, DBNs were used on the SS-BoWs to learn high-level features. Experiments on 3D shape recognition and retrieval demonstrated significant improvements compared to using low-level descriptors only. In [72] Bu et al. extended their work in [71] to a GPU based implementation to accelerate the computations and used it for correspondence and symmetry detection tasks where the proposed framework proved to achieve better performance.

Motivated by the HKS performance in the extracting low-level features, Xie et al [73] used HKS to be employed as a low-level descriptor at multi-scales. The result was fed to AEs to learn discriminative results for the 3D shape retrieval task. To enhance the performance of the features representations, Fisher discriminative analysis was also applied. Experiments proved the robustness of this model against deformations. In [74], Han et al. proposed what is called *Mesh Convolutional Restricted Boltzmann Machines* (MCRBMs) to learn the discriminative hierarchical features of 3D meshes. The proposed model was able to learn both the local and global features of the 3D objects. The structure of the local features was preserved by using the *Local Function Energy Distribution* (LFED). An extension, a deeper model composed of multiple stacked MCRBMs, was tested in the context of shape retrieval and correspondence. This model outperformed state-of-art models such as [13] and [38].

Most of the DL models employed in the previous methods fall under the unsupervised learning methods category because supervised methods tend to learn hierarchical abstractions about the raw data. However, presenting 3D data with descriptors is indeed a form of abstraction. That is why supervised methods might not produce informative features because it would learn abstractions of the abstractions which might lead to a loss of the actual properties of the shapes if the descriptor representation is very simple/abstract. That is where unsupervised methods are more suitable for such representation to learn the hidden patterns or grouping in the input data. However, in some cases, the descriptors can provide rich information on which the convolution operation can be effective to learn the hierarchical features of the input representations such as [74]. These methods can still be combined with unsupervised models. In short, the choice of the DL model on descriptor representations is dependent on how rich the descriptor.

3.1.2 Deep learning architectures based on 3D data projections

One of the first attempts towards learning the features of 3D data by projecting them into 2D planes was presented by Zhu et al. in [75]. The proposed pipeline started by some data pre-processing where translation, scaling and pose normalization were applied on each 3D model. Then, various 2D projections were applied on each processed 3D model to feed it to a stack of RBMs to extract the features of different projections. Then, an AE was used to generate

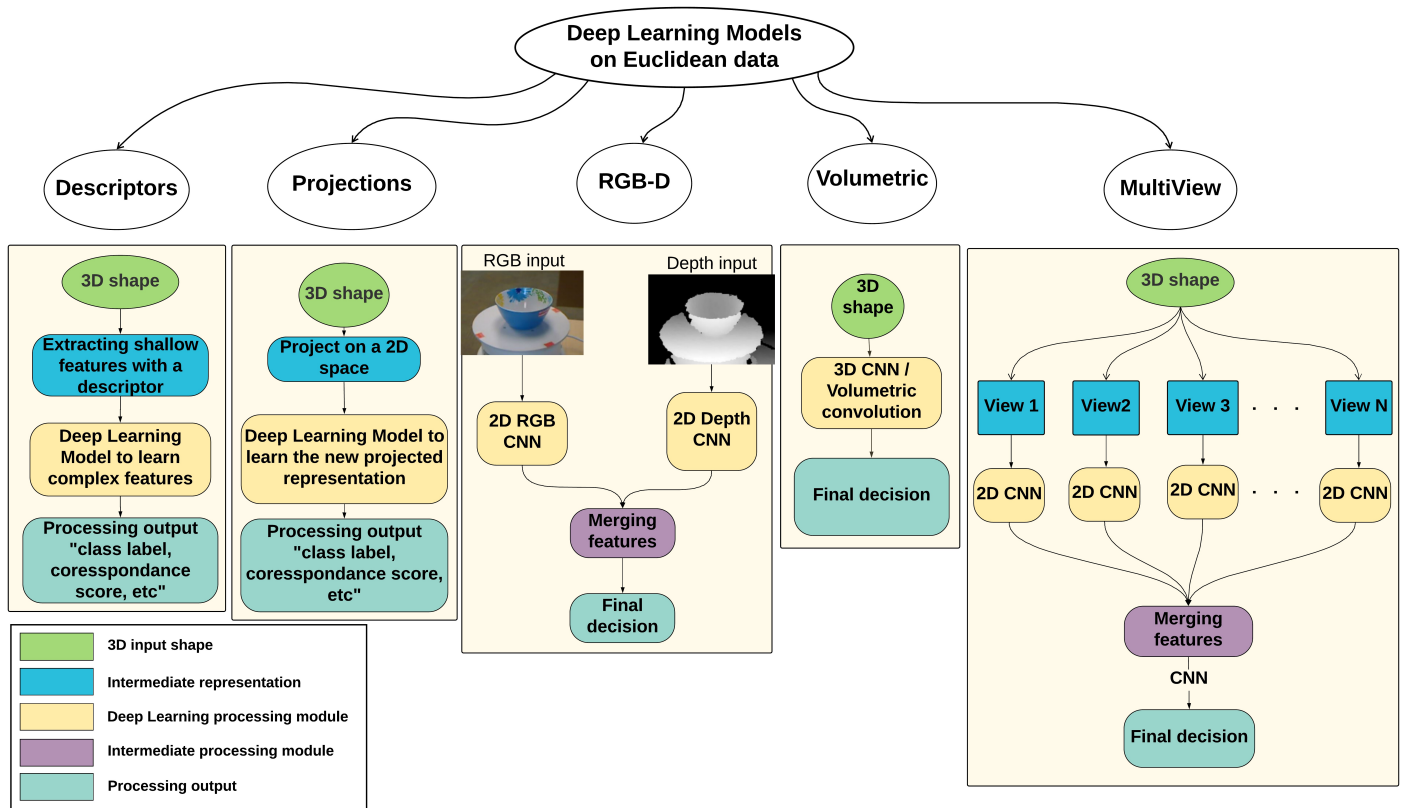


Figure 2: DL models on various Euclidean representations for 3D data.

a global representation of 3D objects for retrieval tasks. The experiments showed that this framework performed better than global descriptor-based techniques. The performance was boosted by combining local representations with the learned global ones. In this context, Shi et al. [48] proposed *DeepPano*. *DeepPano* refers to extracting 2D panoramic views from 3D objects by employing a cylindrical projection around the principal axis of the 3D object. 2D classical CNN architecture was used to train the model except for that a row-wise max-pooling layer was inserted between the Conv and FC layer to make the learnt features invariant to rotations around the principal axis. The proposed network consisted of four Conv layers, one row-wise max-pooling layer, two FC layers and one softmax layer at the top of the network. The proposed model was tested on 3D object recognition and retrieval tasks where it proved its effectiveness in comparison with previous models. Sinha et al. in [10] proposed *geometry images* where 3D objects were projected into 2D grid so that the classical 2D CNNs can be employed as shown in figure 2. The proposed method created a planner parametrization for 3D objects by using aplanic parametrization on a spherical domain to learn the 3D shapes surfaces. Then, the constructed geometry images were served as inputs to classical CNN architecture to learn the geometric features of the 3D objects. As a pre-processing step, data augmentation, scaling, rotation and translation operations were performed to increase the size of the training data and to provide some variety. The geometry images framework was tested on various datasets: *ModelNet10*, *ModelNet40*, *McGill11*, *McGill2*, *SHREC1* and *SHREC2*

on classification and retrieval tasks. Results showed that geometry images produced comparable results to the state-of-art methods [13], [23], [48]

Motivated the results achieved by the projection methods, Cao et al. [47] proposed representing 3D shapes by projecting a 3D object onto a spherical domain centered around its barycenter producing a set of cylindrical patches. The proposed model uses the projected cylindrical patches as an input to pre-trained CNNs. Two complementary projections were also used to better capture the 3D features. The first complementary projection captures the depth variations of the 3D shapes while the second captures the contour information embedded in different projections from different angles. The proposed model was used for 3D object classification task where it was tested on multiple datasets producing comparable results to previous methods. Similar to the previous work, Sfikas et al. [76] proposed to represent 3D objects as panoramic views extracted from normalized posed 3D objects. Initially, 3D objects are preprocessed to normalize their poses using SYMPAN [77] method and then panoramic views are extracted to be combined and fed to CNN to perform classification and retrieval tasks. While being similar to the previous models, this methods enhanced the accuracy when tested on *ModelNet10* and *ModelNet40* datasets. An extension to this model was introduced in [77] where an ensemble of CNNs was used for the learning process. This extension produced very high results when tested on the aforementioned datasets.

Projection-based representations are simple yet effective for learning 3D objects using 3D DL methods. The geometric

properties of the shape is lost due to the projections that is why in the previous work, researchers are trying to combine more than one projection representation to compensate for the missing information. Although 2D DL models can be directly applied on this representation, the networks usually require more fine-tuning than operating directly on the raw 3D data representation which might be tailored to the training data specifically and cause a shortage when tested on new unseen data.

3.1.3 Deep learning architectures on RGB-D data

Due to the availability of RGB-D sensor data, multiple research efforts were directed towards leveraging the available data to exploit it for several tasks. One of the first approaches in this direction was proposed by Socher et al. in [78], where the authors presented a pipeline of convolution and recursive neural networks to process both the color images and depth channels of the RGB-D data. Two single-layer CNNs were used to learn the feature representations from the RGB-D data. The resulted descriptor was fed to a set of RNNs that were initialized with random weights. The results from the RNNs were combined and merged to be used as an input to a softmax classifier. This framework was used for house-old object classification where it showed accurate performance. Researchers continued to use the power of CNNs to learn the RGB-D data features. In [79], Couprie et al. proposed a multi-scale CNN for the semantic segmentation on indoor RGB-D scenes. As the name implies, the proposed network learned the RGB-D data at multiple scales (three different scales). The network is mainly composed of two parallel CNNs where the first CNN is responsible for classifying the objects in the scene and the results of the second CNN are forwarded to a classifier to compute the class label prediction score. The final class label was decided by using the results from the classifier along with the segmented super-pixels of the scene. As a pre-processing step in this model, the RGB-D images are normalized to zero mean and the depth information is added as the fourth pixel to the RGB images and inputted to the CNNs. This method produced better accuracy by 6% than previous models and computationally is very efficient. The takeaway from this method is that despite the simplicity of the use of the CNN combined with depth, the result is much better compared to handcrafted features. Also, this method demonstrates the substantial importance of the depth information for the segmentation application, as it is a key factor for separation among objects. However, the CNN here seems to learn the class object only without learning the geometry of the shape.

Inspired by the results of the two-stream network proposed in [79], researchers started exploiting the same concept introducing some novel modifications. Instead of using the networks for two different learning tasks (classification and segmentation), researchers started processing the depth information and the color information separately using a different network, which started to be a common practice in processing RGB-D data as shown in the pipeline depicted in figure 2 under the RGB-D data representation. Eitel et al. in [80] proposed to use a two-stream CNN for 3D object recognition on RGB-D data as illustrated in Figure 3. One CNN stream processes the RGB color information and the

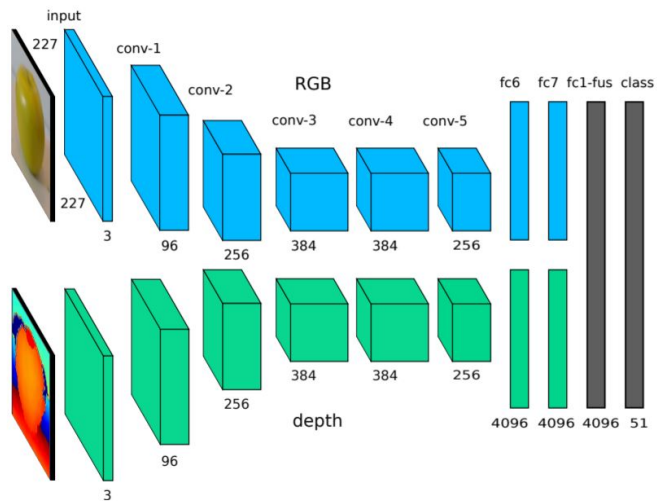


Figure 3: Two-stream CNNs for 3D object recognition on RGB-D data [80]

other stream is for processing the depth. Each of the two CNN has five Conv layers and two FC layers. Each network was trained separately and then the results were fused in the FC layer and the softmax classifier to decide on the object's class. This method outperformed previous existing methods and demonstrated a promising performance for object recognition in real-world noisy environments. Feng et al. [81] proposed an ensemble of AEs for the 3D shape retrieval task using only one RGB-D model. Each AE was trained using the Stochastic Gradient Descent algorithm on a dataset of different CAD models. Because of the difference between the input test data and the data that was used during the training stage, the output scores of the AEs are then forwarded to what they called *Domain Adaption Layer* (DAL) to rank the retrieved scores. This method enhanced the performance in comparison with other related methods.

Alexandre [82] combined the concept of transfer learning and CNNs together to train 4 CNNs separately. Transfer learning is used between CNNs for RGB-D data object recognition. In this model, each channel of the four channels in the RGB-D data was processed using a separate CNN and the weights were transferred from each network to another. Experiments indicated that this method boosted the performance which implies that the depth information carries valuable information about the 3D shape. Which pushed Schwarz et al. in [83] to explore the transfer learning concept for the object classification task on RGB-D data. In this model, RGB-D data was rendered from a canonical perspective and the resulted depth was colored based on the distance from the object's centre. The CNN employed in this model was a pre-trained CNN for object categorization. The output of the network's two last layers was used as the object descriptor, which was forwarded to SVMs to learn the object's class. The pre-training stage enables the model to extract better features which helps boost the performance.

Deep learning proved to be effective in learning RGB-D data despite the simplicity of the models. Moreover, processing the depth channel separately conveys that the depth has valuable information about the 3D signal that contributes the whole learning process. However, these methods don't

learn the full geometry of the 3D object and can only infer some of the 3D properties based on the depth. Later works we overview, examine the full volumetric representation of the 3D shape rather than using the flat 2D images of color and the depth informations.

3.1.4 Deep learning architectures on volumetric data

Some efforts were directed towards processing the 3D volumetric representations of 3D objects to exploit the full geometry of the object. *ShapeNet* [13] is the first DL model exploiting the geometry of 3D objects represented as voxels. The input object is represented as a 30x30x30 binary tensor indicating whether the voxel is part of the 3D object or not. A Convolutional Deep Belief Net [84] concept was adapted from 2D DL to model 3D objects (CDBN). CDBNs can be seen as a variation of DBNs where convolution is also employed to reduce the number of parameters due to the weight sharing property. That is why CDBNs are used to model and learn the joint probability distribution over voxels representing different object categories with a small number of parameters. *ShapeNet* is composed of five layers (one input layer, three convolution layers and one output layer). The proposed network was initially pre-trained. In the pre-training stage, the network was trained in a layer-wise fashion where the first four layers are trained using the Contrastive Divergence method and the last layer was trained using the Fast Persistent Contrastive Divergence. During the test stage, the input is provided as a single depth map for the 3D object, which is then converted into a voxel grid representation. *ShapeNet* was tested on three different tasks: 3D shape classification and retrieval, next-based view prediction and view-based recognition. The authors provide two results for testing on *NYU v2* for the object recognition task; the first one applies the data directly to the network and the other one involves fine-tuning on real-world data. The fine-tuned network produces better results suggesting that it is a performance-boosting step. Although *ShapeNet* was the first network to exploit 3D volumetric data directly in deep learning, it is imposing many constraints. The additional dimension in the convolution kernel results in a computationally intractable model that can hardly process large sized or high-resolution data. Also, the network is trained on isolated view of fixed size voxels without any additional information or background clutter which makes the learning process hard. Despite these limitations, this network produces impressive results given that it is operating on low-resolution voxels. Also, besides presenting *ShapeNet* in [13], the authors also presented *ModelNet* dataset which is described in details in section 4.1. The availability of 3D CAD labelled models opened the door for more experiments and boosted the research in this area.

Maturana and Scherer in [12] exploited the concept of 3D convolution and proposed *VoxNet* to perform 3D object recognition on different 3D data representations: RGB-D data, LIDAR point clouds and 3D CAD models. The convolution in *VoxNet* followed the 2D Convolution except for the filter where a 3D filter was used instead of a 2D filter. The network architecture was constructed using one input layer, two Conv layers, one pooling layer and two FC layers. The input data was constructed as a volumetric occupancy grid of 32x32x32 voxels and

it was fed to the network that was trained using the Stochastic Gradient Descent (SGD) with momentum. Experiments showed that *VoxNet* outperforms *ShapeNet* when tested on *ModelNet10*, *ModelNet40* and *NYUv2* dataset for the classification task when the networks are trained from scratch. However, *ShapeNet* outperforms *VoxNet* when tested on *NYUv2* when the pre-trained model for *ModelNet10* is used. Motivated by the promising performance of *VoxNet*, Seaghat et al. [85] modified the architecture of the *VoxNet* to incorporate the orientation of the 3D object in the learning process. This enhanced the classification results on the *ModelNet10* dataset. To learn the 3D data representations using unsupervised techniques, the authors proposed 3D-GAN [86] to implicitly learn the features of 3D objects from the probabilistic latent space using the adversarial discriminator. The adversarial discriminator learns to capture the structure of 3D objects with the ability to identify whether it is real or synthesized. This carried a discriminative semantic information about 3D objects which is effective for modelling 3D objects and generating synthetic data as shown in the experiments.

The great advancements in the 2D very deep architectures motivated Brock et al. [11] to adopt such models for 3D object classification on *ModelNet10* and *ModelNet40* datasets. The authors proposed *Voxception-ResNet* (VRN) very deep model. As the name implies, VRN relied on Inception architectures [6] [87]. In addition to adopting the batch normalization methods [6], [88] and stochastic network depth techniques [89]. VRN is composed of 45 layers deep, which required data augmentation for the training process. VRN is similar to *VoxNet* in a sense that they both adopt ConvNet with 3D filters but VRN is very deep compared to *VoxNet*, which achieved a significant improvement by 51.5% in the classification task on *ModelNet* datasets which marks the state-of-art results on this dataset. Despite the effectiveness of this method, it has a complex architecture and requires a significant amount of data augmentation to avoid the over-fitting problem that can result from the deep architecture of a small dataset. These constraints are limiting and can not easily be achieved. Xu and Todorovic proposed the beam search model to learn the optimal 3D CNN architecture to perform classification on *ModelNet40* dataset [90]. The proposed model identifies the 3D CNN number of layers, number of nodes, connectivity and the training parameters as well. The model starts with a fairly simple network (two Conv layers and one FC layer). The beam search method starts with this architecture and extends it to build the optimal 3D CNN model by either adding a new Conv filter or adding a new Conv layer. The beam search model is trained in a layer-wise fashion where the standard Contrastive Divergence method is used to train Conv layers and the Fast Persistent Contrastive Divergence is used to train the FC layer. Once one layer is learned, the weights are fixed and the activation parameters are transferred to the next layer. The proposed method produced significant results in the classification task on *ModelNet40* dataset.

In an attempt to learn the 3D features at different scales using 3D CNNs, Song and Xiao in [91] proposed *DeepSlidingShapes* model to perform 3D object recognition and classification on *ModelNet* dataset. the authors

in figure 5. Two different setups to capture the 3D objects multi-views were tested. The first one rendered 12 views for the object by placing 12 equidistant virtual cameras around the object while the second setup included 80 virtual views. MVCNN was pre-trained using *ImageNet1K* dataset and fine-tuned on *ModelNet40* [13]. The proposed network has two parts, the first part is where the object’s views are processed separately and the second part is where the max pooling operation is taking place across all the processed views in the view-pooling layer, resulting in a single compact representation for the whole 3D shape. In the view-pooling layer, the view with the maximal activation is the only one considered while ignoring all the other views with non-maximal activations. This means that only few views are contributing towards the final representation of the shape which causes a loss of the visual information. To overcome this problem,

Experiments showed that the MVCNN with the max-view pooling layer outperformed ShapeNet [13] on classification and retrieval tasks by a remarkable margin. In [97] Johns et al. exploited multi-view data representation using CNNs by representing 3D objects by a set of 2D image pairs under unconstrained camera trajectories. The proposed method classifies each pair separately and then weight the contribution of each pair to get the final result. The VGG-M architecture was adopted in this framework consisting of five Conv layers and three FC layers. The views of the 3D objects are represented as either depth images or grayscale images or both. This model outperformed MVCNN proposed by Su et al. [23] and voxel-based ShapeNet architectures [13].

The efficiency of multi-view DL models pushed researchers to investigate more GPU-based methods to learn multi-view 3D data features. This is what pushed Bai et al. [98] to propose a real-time GPU-based CNN search engine for multi 2D-views of 3D objects. The proposed model called *GIFT* utilizes two inverted files: the first one is for accelerating the multi-view matching process and the second one is for ranking the initial results. The processed query is completed within one second.

GIFT was tested on a set of various datasets: *ModelNet*, *PSB*, *SHREC14LSGTB*, *McGill* and *SHREC’07* watertight models. *GIFT* produced a superior performance compared to state of art methods.

The efforts to learn multi-view 3D data representations kept evolving and in [99], Zanuttigh and Minto proposed a multi-branch CNN for classifying 3D objects. The input to this model is a set of rendered depth maps from multiple points of views for the 3D object. Each CNN branch consists of five Conv layers to process one depth map producing a classification vector. The resulted classification vectors are then fed to a linear classifier to identify the class of the 3D object. The proposed model produced comparable results to the state-of-art. In [100], Want et al. proposed the recurrent view-clustering and pooling layers based on the dominant sets. The key concept in this model is to pool similar views and recurrently cluster them to build a pooled feature vector. Then, the constructed pooled feature vectors are fed as inputs in the same layer in a recurrent training fashion in the recurrent clustering layer. Within this layer, a view similarity graph is computed whose nodes represent the feature vec-

tors and the edges represent the similarity weights between the views. Within the constructed graph, the similarities and dissimilarities between different views are exhibited which is very effective in the 3D shape recognition task. The proposed model achieved a highly comparable result to the state-of-art methods [13] [23] as shown in table ?? . Driven the advances in the multi-view DL models, Qi et al [101] provided a comparison study between multi-view DL techniques and volumetric DL techniques for the object recognition task. As part of the study, the authors proposed a *Sphererendering* approach for filtering multi-resolution 3D objects at multiple scales. With data augmentation, the authors managed to enhance the results of MVCNNs on *ModelNet40*.

Multi-view representation proved to perform slightly better than volumetric representation with less computational power needed. However, there are some challenges imposed with this representation. The sufficient number of views and the way they were acquired is a critical factor for representing the 3D shape. Also, the multi-view representation doesn’t preserve the intrinsic geometric properties of the 3D shape. This is what pushed towards defining new notion of convolution operating on the 3D shape to capture the intrinsic property of the shape.

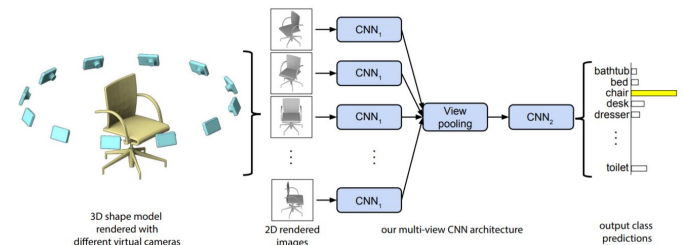


Figure 5: MVCNN architecture [23] applied on multi-view of 3D objects without a specific order.

3.1.6 Deep learning architectures on hybrid data representations

Some efforts towards combining various 3D data representations to exploit the advantages that each representation brings. Recently, Wang et al. in [102] where each 3D object is represented by a pair of multi-views and 2D sketch. The learning model is composed of Siamese CNNs where are two identical sub-convolutional networks; one for processing the multi-views input and the other one is for processing the 2D sketches. Each of these network consisted of three Conv layers where each of them was followed by a max pooling layer and then a FC layer at the top. The networks were trained separately using the Stochastic Gradient Descent method. The proposed model was tested on SHREC’13 dataset for 3D shape retrieval and achieved competitive results compared to previous methods in the literature. Wang et al. continued their investigations for hybrid 3D data representations and in [103], the authors proposed the Convolutional Auto-Encoder Extreme Learning Machine (CAE-ELM) 3D descriptor which combines the learning power of ConvNets, AEs and Extreme Learning Machine (ELM) [104]. ELM is an efficient unsupervised learning technique that learns high-level discriminative features about the input

data. ELM is faster than most of DL models [105] which is practical for processing large-scale 3D data. The input to the CAE-ELM architecture is two data representations: voxel data and Signed Distance Field data (SDF). Voxel data describes the structure of the 3D object while the SDF extracts local and global features about the 3D object. CAE-ELM was tested on *ModelNet10* and *ModelNet40* datasets for classification tasks and achieved a superior performance compared to previous methods. CAE-ELM is considered as a hybrid approach that exploits the structure of the 3D objects in addition to 3D descriptors. In the work of Ben-Shabat et al. [106], the authors proposed a novel 3D point cloud representation called *3D Modified Fisher Vectors* (3DmFV) which is a DL model that uses a hybrid data representation of the discrete structure of a grid with the continuous generalization of Fisher vectors to represent the 3D data. The hybrid input data is processed using deep ConvNet for classification and part segmentation tasks. 3DmFV has two modules: the first one converts the input point cloud to the 3D modified Fisher vector (FV) which can be considered as a descriptor-based representation and the second one is the DL module represented in the CNN. FV data representation enables the proposed framework to be invariant to order, structure and the sample size of the input data. The network architecture is composed of an inception module [87], max-pooling layers and four FC layers on top. The network achieved competitively compared to the state-of-art methods.

Inspired by the performance of 3D convolution and 2D multi-view CNNs, some work examined the fusion of both representations. Hedge and Zadeh [107], proposed to fuse the volumetric representations (i.e., voxels) and 2D representation (i.e., 2D views) for the object classification task. The authors examined different models for processing the data for *ModelNet* classification. The model one was a combination of both modalities (3D and 2D) while using two 3D CNNs for processing the 3D voxels and AlexNet for processing the 2D views. The other experiments were carried by processing the 3D voxels only and compare it with the performance of AlexNet on the 2D views. Experiments showed that that network that combined both modalities called *FusionNet* performed the best. However, the multi-view network performed better than the volumetric CNNs. Although Brock et al. [11] achieved the state-of-art results on *ModelNet* classification, *FusionNet* achieved comparable results with no need for the data augmentation or the very heavy computations needed in Brock’s model. This implies that practically employing 2D and 3D representations surpass the volumetric methods with less computations.

3.2 Deep learning architectures on 3D non-Euclidean structured data

The second type of 3D DL approaches is the non-Euclidean approaches that try to extend the DL concept to the geometric data. However, the nature of the data is imposing challenges on how to perform the main DL operations such as convolution. A number of architectures that tried to extend DL to the 3D geometric domain were proposed. Some of these architectures address 3D point clouds to learn the geometry of the 3D shape and use it for modeling

tasks. Results encouraged researchers to leverage the surface information provided in 3D meshes where the connectivity between vertices can be exploited to define local pseudo-coordinates to define a convolution-like operation on 3D meshes. At the same time, some efforts were directed towards investigating graph-based 3D data attempting to leverage the spectral properties of graphs to define intrinsic descriptors to be used in the DL framework. In this section, we will go over the latest innovations in applying DL on non-Euclidean 3D data.

3.2.1 Point clouds

Point clouds provide an expressive, homogeneous and compact representation of the 3D surface geometry without the combinatorial irregularities and complexities of meshes. That is why point clouds are easy to learn from. However, processing point clouds is tricky due to its dual nature. Point clouds can be seen as a Euclidean-structured data when considering a point with respect to its neighborhood (a subset of points) such that the interaction among the points forms a Euclidean space with a distance metric which is invariant to transformations such as translation, rotation. However, considering the global structure of the point cloud, it is an unordered set of points with no specific order which imposes the irregular non-Euclidean nature on the global structure of the data.

Some recent works have considered point clouds as a collection of sets with different sizes. Vinyals et al. in [108] use a read-process-write network for processing point sets to show the network ability to learn how to sort numbers. This was a direct application of DL on unordered set for the NLP application. Inspired by this work, Ravanbakhsh et al. [109], proposed what they called the permutation equivariant layer within a supervised and semi-supervised settings. This layer is obtained by parameter-sharing to learn the permutation invariance as well as rigid transformations across the data. This network was used to perform 3D classification and MNIST digit summation. Although this network is relatively simple and has a linear time complexity in the size of each set, it didn’t perform well on the 3D classification task on *ModelNet* dataset. A deeper version of this model was extended in [110] where the proposed *DeepSet* framework produced comparable results to the state-of-art method in the 3D classification task on *ModelNet* dataset. Due to the permutation invariance property that the permutation equivariant layer is bringing to the previous models. [111] also used a similar layer with a major difference as the permutation equivariant layer is max-normalized.

PointNet [112] is the pioneer in making a direct use of the point cloud as an input where each of its points is represented using the (x, y, z) coordinates. As a pre-processing step, input and feature transformations are applied to the input and then fed to the *PointNet* architecture. *PointNet* is composed of three main modules: a Spatial Transformer Network (STN) module, an RNN module and a simple symmetric function that aggregates all the information from each point in the point cloud. The STN canonicalizes the data before feeding them to the RNN and learns the key points of the point cloud which approximately correspond to the skeleton of the 3D object. Then comes the RNN

module which learns the point cloud as a sequential signal of points and by training this model with randomly permuted sequences, the RNN becomes invariant to the sequence of the input order of the point cloud's point. Lastly, the network aggregates all the resulted point features using the max-pooling operation which is also permutation invariant. *PointNet* proved that it is robust against partial data and input perturbation. It was tested on classification and segmentation tasks where it proved to produce results comparable to the state-of-art as shown in table ??.

Despite the competitive results achieved by *PointNet*, it does not take a full advantage of the point's local structure to capture the detailed fine-grained patterns because of aggregating all the point features together. To address this point, *PointNet++* [113] builds on *PointNet* by recursively applying it on a nested partitioning of the input point set. Despite capturing more features, the resulted architecture is complicated which increases the size of the higher features and reduce the computational speed.

Instead of operating directly on the point clouds structure, Kd-Networks by Klokov et al. [114] proposes to impose a kd-tree structure of the input point cloud to be used for learning the shared weights across the points of the tree. Kd-tree is a feed-forward network that has learnable parameters associated with the weights of the nodes in the tree. This model was tested for shape classification, shape retrieval and shape part segmentation producing competitive results. Following the same concept of not working directly on the point cloud structure, Roveri et al. [115] proposed to extract a set of 2D depth maps from different views of the point cloud and process them using *ResNet50* [116]. The proposed framework is composed of 3 modules. The first module is responsible of learning k directional views of the input point cloud to generate the depth maps accordingly in the second module. The third and last module is processing the generated k depth maps for object classification. The innovation of this framework is mainly focus on automatically transforming unordered point clouds to informative 2D depth maps without the need to adapt the network module to account for permutation invariance and different transformations of the input data.

Recently, some work has been done on unsupervised learning on point clouds. In *FoldingNet* [117], Yang et al. proposed to use AE for modelling different 3D objects represented as point clouds by a novel folding-based decoder than deforms a 2D canonical grid into the underlying surface of the 3D point cloud. *FoldingNet* is able to learn how to generate cuts on the 2D grid to create 3D surfaces and generalize to some intra-class variations of the same 3D object class. An SVM was used on top of this *FoldingNet* to be used for 3D classification where it proved to perform well with the learned discriminative representation for different 3D objects. *FoldingNet* achieved high classification accuracy on *ModelNet40*. Another unsupervised model was proposed by Li et al. called *SO-Net* [118]. *SO-Net* is a permutation invariant network that can tolerate unordered point clouds inputs. *SO-Net* builds that spatial distribution of the points in the point cloud using *Self-Organizing Maps* (SOMs). Then, a hierarchal feature extraction on the points of the point cloud and the SOM nodes is employed resulting in a single feature vector that represents the whole point

cloud. Local feature aggregation happens according to an adjustable receptive field where the overlap is controlled to get more effective features. *SO-Net* was tested on classification and segmentation tasks producing promising results highly comparable to the state-of-art as shown in table ??.

As noticed in all the previously proposed methods, the main problem in processing point clouds is the unordered structure of this representation where researchers are trying to make the learning process invariant to the order of the point cloud. Most of these methods resorted to clustering techniques to opt for similar points and process them together.

3.2.2 Graphs and meshes

The ideal representation for graphs and meshes is the one that can capture all the intrinsic structure of the object and also can be learned with the gradient descent methods due to their stability and frequent usage in the CNNs. However, learning such irregular representations is a challenging task due to the structural properties of such representations. Motivated by the success of CNNs in a broad range of computer vision tasks, recent research efforts were directed towards generalizing CNNs to such irregular structures. Analyzing the properties of such data shows that meshes can be converted to graphs as discussed in section 2.2.2. Hence, the models proposed for graphs can be employed on mesh-structured data but not vice versa. Most of the existing work addresses the graph-structured data explicitly with some few works were tailored towards mesh representations. Here we overview recent works on each representation providing a broad classification for the existing methods based on the used approach.

Graphs: Studying the structural characteristics of both graphs and meshes suggests that the proposed learning methods for graphs are also applicable on meshes. Existing methods for Graph Convolutional Neural Networks (GCNN) can be broadly categorized into two main directions: spectral filtering methods and spatial filtering methods. Here we discuss the underlying concept behind each method and overview the work done in each direction. The distinction between both directions is in how the filtering is employed and how the locally processed information is combined.

- *Spectral filtering methods.* The notion of spectral convolution on graph-structured data was introduced by Bruna et al. in [119] where the authors proposed Spectral CNN (SCNN) operating on graphs. The foundation of the spectral filtering methods is to use the spectral eigen-decomposition of the graph Laplacian to define a convolution-like operator. This redefines the convolution operation in the spectral domain where the main two core stones are analogous: the patches of the signal in the Euclidean domain correspond to the functions defined on the graph nodes e.g. features, mapped to the spectral domain by projecting on the eigenvectors of the graph Laplacian and the filtering operation itself in the Euclidean domain correspond to scaling the signals in the eigenbasis. This definition implies that convolution is a linear operator that commutes with

the Laplacian operator meaning that this is applicable only to the graph weights are given by the eigenvectors if the graph Laplacian [18]. Despite the innovation aspect of Bruna’s model, it has serious limitations due to being basis dependent and computationally expensive. Being basis dependent means that if the spectral filter’s coefficients were learned w.r.t a specific basis, applying the learned coefficients on another domain with another basis will produce very different results as illustrated in [18]. The other limitation of being computationally costly arises from the fact that spectral filtering is a non-local operation that involves data across the whole graph besides that the graph Laplacian is expensive to compute. This constitutes a computational burden towards generalizing to other basis and processing large-scale graphs.

The work in [120] addressed the basis dependency problem by constructing a compatible orthogonal basis across various domains by using a joint diagonalization. However, this required a pre-knowledge about the correspondence between the domains. In some applications such as social networks, this is a valid assumption because the correspondence can be easily computed between two-time instances in which new edges and vertices have been added. However, applying this on meshes is rather unreasonable because finding correspondence between two meshes is challenging task on its own, so the assuming the knowledge of correspondence between domains in such case is unrealistic [18]. Since the non-local nature of the spectral filtering and the need to involve all the graph data in the processing, recent works proposed the idea of approximation to produce local spectral filters [121] [122]. What these methods propose is to represent the filters via a polynomial expansion instead of directly operating on the spectral domain. Defferrard et al. in [121] performed local spectral filtering on graphs by using Chebyshev polynomials to approximate spectral graph filters. The features yielding from the convolution operation are then coarsened using the graph pooling operation. Kipf and Welling [122] simplified the polynomial approximation proposed in [121] and used a first-order linear approximation of the graph spectral filters to produce local spectral filters which are then employed in a two-layer GCNN. Each of these two layers uses the local spectral filters and aggregates the information from the immediate neighbourhood of the vertices. Note that the filters proposed in [121] and [122] are employed on r - or 1-hop neighbourhood of the graph which boils down these constructions into the spatial domain.

Driven by the success of the local spectral filtering models, Wang et al. [123] proposed to leverage the power of spectral GCNNs in the pointNet++ framework [113] to process unordered point clouds. This model fuses the innovation of the pointNet++ framework with local spectral filtering while addressing two shortcomings of these models independently. So, instead of processing each point independently

in the point clouds as proposed in pointNet++, this model uses spectral filtering as a learning technique to incorporate the structural information in the neighbourhood of each point. Moreover, instead of using the greedy winner-takes all method in the graph max pooling operation, this method adopts a recursive pooling and clustering strategy. Unlike the previous spectral filtering methods, this method requires no pre-computation and is trainable in an end-to-end manner which allows building the graph dynamically and computing the graph Laplacian and the pooling hierarchy on the fly unlike [119], [121], [122]. This method achieved state-of-art recognition results on diverse datasets as depicted in table ??.

- *Spatial filtering methods.* The concept of graph spatial filtering started in [124] when GNNs were first proposed as an attempt to generalize DL models to graphs. GNNs are simple constructions that try to generalize the notion of spatial filtering on graphs via the weights of the graph. GNNs are composed of multiple layers where each layer is a linear combination of graph high-pass and low-pass operators. This formulation suggests that learning the graph features is dependent on each vertex’s neighborhood. Similar to Euclidean CNNs, a non-linear function is applied to all the nodes of the graph where the choice of this function vary depending on the task. Varying the nature of the vertex non-linear function allowed for rich architectures [125], [126], [127], [128], [129]. Also, analogous to CNNs, pooling operation can be employed on graph-structured data by graph coarsening. Graph pooling layers can be done can interleave the graph learning layers. In comparison with the spectral graph filtering, spatial filtering methods have two key points which distinguish them from spectral methods. Spatial methods aggregate the feature vectors from the neighborhood nodes directly based on the graph topology considering the spatial structure of the input graph. The aggregated features are then summarized via an additional operation. The GNN framework proposed in [124], [130], proposed to embed each vertex in the graph into a Euclidean space with an RNN. Instead of using the recursive connections in the RNN, the authors used a simple diffusion function for their transition function, propagating the node representation repeatedly until it is stable and fixed. The resulting node representations are considered as the features for classification and regression problems. The repeated propagation for node features in this framework constitutes a computational burden which is alleviated in the work proposed by Li et al. [125]. The authors proposed a variant of the previous model which uses the gated recurrent units to perform the state updates to learn the optimal graph representation. Bruna et al. in [119] imposed the spatial local receptive field on GNN to produce their local spatial formulation of GNN. The main idea behind the local receptive field is to reduce the number of the learned parameters by grouping similar features based on a similarity measure [131],

[132]. In [119], the authors used this concept to compute a multi-scale clustering of the graph to be fed to the pooling layer afterwards. This model imposes locality on the processed features and reduces the number of processed parameters. However, it is not performing any weight sharing similar to 2D CNNs. Niepert et al. in [133] performs spatial graph convolution in a simple way by converting the graph locally into sequences and feeding these sequences into a 1D CNN. This method is simple but requires an explicit definition for the nodes orders of the graphs in a pre-processing step. In [134], the authors provided a detailed study proving that spectral methods and spatial methods are mathematically equivalent in terms of their representation capabilities. The difference resides in how the convolution and the aggregation of the learned features are performed. Depending on the task, the architecture of the GCNN (spectral or spatial) is formed where the convolution layers may be interleaved with coarsening and pooling layers to summarize the output of the convolution filters for a compact representation of the graph. This is crucial in classification applications where the output is only one class inferred from the learned features [119]. Some other applications require a decision per node such as community detection. A common practice in such cases is to have multiple convolution layers that compute the graph representations at the node level [135], [136], [137]. All these GCNNs are end-to-end differentiable methods that can be trained in supervised, semi-supervised or reinforcement learning techniques.

Meshes: On the Euclidean domain, the convolution operation is simply passing a template at each point on the spatial domain and recording the correlation of the template with the function defined at this point. This is feasible due to the shift-invariance property on the Euclidean domain. Unfortunately, this is not directly applicable on meshes due to the lack of the shift-invariance property. This is what pushed towards defining local patches that represent the 3D surface in a way that allows performing convolution. However, due to the lack of the global parametrization on the non-Euclidean data, these patches are defined in a local system of coordinated locally meaning that these patches are also position-dependent. Recently, various non-Euclidean CNNs frameworks were proposed. The main schema used by these frameworks is very similar except for how the patches are defined mostly. The local patches are defined either by handcrafting them or by depending on the connectivity of the vertices while using the features of the 1-hop neighborhood as the patch directly [15]. The convolution employed in such frameworks is very similar to the classical 2D convolution where it is basically an element-wise multiplication between the convolution filter and the patch and summing up the results. This is because the patches extracted by such frameworks boils down the representation into 2D where the classical convolution can be employed.

Geodesic CNN [138] was introduced as a generalization of classical CNNs to triangular meshes. The main idea of

this approach is to construct local patches in a local polar coordinates. The values of the functions around each vertex in the mesh are mapped into local polar coordinates using the patch operator. This defines the patches where the geodesic convolution is employed. Geodesic convolution follows the idea of the multiplication by a template, however, the convolution filters in this framework are subjected to some arbitrary rotations due to the angular coordinate ambiguity. This method opened the door for new innovations on extending CNN paradigm to triangular meshes. However, this framework suffers from multiple drawbacks. First, it can only be applied on triangular meshes where it is sensitive to the triangulation of the mesh and it might fail if the mesh is extremely irregular. Second, the radius of the constructed geodesic patch has to be small with respect to the injectivity radius of the actual shape to guarantee that the resulted patch is topologically a disk. Third, the rotations employed on the convolution filters makes the framework computationally expensive which limits the usage of such framework. Anisotropic CNN (ACNN) [139] was proposed to overcome some of the limitations in the geodesic CNN. Compared to the geodesic CNN, ACNN is not limited to triangular meshes and can be also applied to graphs. Also, the construction of the local patches is simpler and is independent on the injectivity radius of the mesh. ACNN uses the concept of spectral filtering where the spatial information is also incorporated by a weighting function to extract a local function defined on the meshes. The learnt spectral filters are applied to the eigenvalues of the anisotropic Laplacian Beltrami Operator (LBO) and the anisotropic heat kernels act as a spatial weighting functions for the convolution filters. This method has shown very good performance for local correspondence tasks. Rather than using a fixed kernel construction as in the previous models, Monti et al. [16] proposed *MoNet* as a general construction of patches. The authors proposed to define a local system of coordinates of pseudo-coordinates around each vertex with weight functions. On these coordinates, a set of parametric kernels are applied on these pseudo-coordinates to define the weighting functions at each vertex. That is why the previous methods [138], [139] can be considered as a specific instances of *MoNet*. Some recent work has been proposed to eliminate the need to explicitly define the local patches on the graphs or meshes such as SplineCNN [15]. SplineCNN is a convolutional framework that can be employed on directed graphs of any dimensionality. Hence, it can also be applied on meshes. Instead of defining the local patches by a charting-based method like the previous methods, SplineCNN uses the 1-hop neighborhood ring features of the graph as the patch where the convolutional filter can operate. The convolutional filter itself is a spatial continuous filter based on B-Spline basis functions that have local support. This framework produces the state-of-art results on the correspondence task while being computationally very efficient. This is due to the local support of the B-Spline basis which makes the computational time independent of the kernel size.

4 ANALYSIS AND DISCUSSIONS

DL methods have been designed and successfully applied on various 3D data representations as discussed in the previous sections. Several approaches have been proposed. We herein discuss the evolution of these models to exploit the depth information on various representations highlighting the strengths and weaknesses of each approach and the tradeoffs imposed on using one approach over the other.

4.1 3D Datasets

Due to the increase in the 3D datasets, we overview below the most recent datasets and their shortcomings.

There are two main categories of data used in the 3D community: real-world datasets and synthetic data rendered from CAD models. It is preferable to use the real-world data; however, real data is expensive to collect and usually suffers from noise and deformation problems. In contrast, synthetic data can produce a huge amount of clean data with limited modelling problems. While this can be seen advantageous, it is quite limiting to the generalization ability of the learned model to the real-world test data. It is also important to note that most 3D datasets are smaller than *ImageNet* [140]. However, some recent 3D datasets are rival to *ImageNet* in size, which is especially important to learn the geometry of the 3D shapes.

ModelNet [13] is the largest dataset for object recognition and classification. It contains roughly 130K annotated CAD models on 662 distinct categories. This dataset was collected using online search engines by querying for each of the categories. Then, the data were manually annotated. *ModelNet* provides the 3D geometry of the shape without any information about the texture. *ModelNet* has two subsets: *ModelNet10* and *ModelNet40*. These subsets are used in a majority of the recently published work as shown in tables ???. In this survey (see section ??), we are providing an extensive analysis of the methods employed on *ModelNet* dataset for recognition and retrieval task highlighting the evolution of DL methods for learning such data.

SUNCG [141] contains about 400K of full room models. This dataset is synthetic, however, each of these models was validated to be realistic and it was processed to be annotated with labelled object models. This dataset is important for learning the scene-object relationship and to fine-tune real-world data for scene understanding tasks. *SceneNet* [142] is also an RGB-D dataset that uses synthetic indoor rooms. This dataset contains about 5M scenes that are randomly sampled from a distribution to reflect the real world. However, not all the generated scenes are realistic and in practice, some of them are highly unrealistic. Still, this dataset can be used for fine-tuning and pre-training. In contrast, *ScanNet* [143] is a very rich dataset for real-world scenes. It is an annotated dataset labelled with semantic segmentation, camera orientation and the 3D information from 3D video sequences taken in real-indoor scenes. It includes 2.5M views, which allows for training directly without pre-training on other datasets, as it is the case with different datasets.

Recently, datasets for 3D meshes started to be present in the 3D computer vision community. The *TOSCA* dataset

provides a high-resolution 3D synthetic meshes for non-rigid shapes. It contains a total of 80 objects in various poses. Objects within the same category have the same number of vertices and the same triangulation connectivity. *TOSCA* provides artistic deformations on the meshes to simulate the real-world deformations of the real scans. *SHREC* adds a variety of artificial noise and artistic deformations to *TOSCA* scans. However, the artificial noise and deformations are not realistic and can't generalize to new unseen real-world data which is a common requirement in all the recent tasks. *FAUST* dataset however, provides 300 real-300 scans for 10 people in various poses.

4.2 Evolution of DL models on Euclidean 3D data representations

Descriptors have been proposed as initial attempts to address the 3D shape analysis problem in combination with classical 2D DL paradigms. While being simple and easy to implement, these models lack the discriminative representation power to learn the 3D features uniquely. However, they are more effective than using shallow descriptors only. Moreover, employing DL on simpler representations of 3D objects encouraged researchers to dig deep into this direction and investigate more. This pushed towards converting 3D data into another sophisticated yet still 2D format where the classical well-researched DL approaches can be employed. This set of methods is the projections-based methods where the intrinsic properties of the 3D shape can be encoded in a simpler 2D format such as in [10]. These methods proved to be effective in classification and recognition tasks, however, still the full geometry of the 3D shapes is not fully exploited and the architecture of the proposed DL models was not enough to answer the 3D research community DL needs. Later work proposed to use the depth information explicitly in RGB-D data. Initial works in this direction sought to treat the depth information as a fourth pixel and stack it to the already existing 3 RGB channels [79]. Although the depth information was not used in the best possible way, the contribution was in the network architecture where a 2 stream CNNs were operating on the stacked RGBD data for the segmentation task. Surprisingly, the use of depth information in this simple manner impressively outperformed previous models on 3D segmentation task. Inspired by this result, researchers tried to adopt the 2D CNN paradigm while processing the depth information separately as in [80]. This enhanced the geocentric encoding of the 3D data and showed clear improvements in the performance. Moreover, processing the RGB signal separately enabled for having fine-tuning on large datasets like *ImageNet* which is very useful in case of limited 3D training data.

Later works shifted towards exploiting the geometry of the full 3D objects directly rather than treating the depth as a 2D mapping of the signal. Various ways are used to represent the 3D signal in this case as: 3D voxel grids [13], octree-based volumetric representation [22] or as 3D volumes created from depth maps [141]. Usually, CNN is used as the DL paradigm employed on such data where the convolution is applied using 3D kernels. These methods significantly performed better than the previous

methods. However, the main drawback of such methods is the prohibitively high computational cost resulting from the cubically increasing number of the 3D convolution and processing every voxel in the 3D space. This imposes the low-resolution constraint on the processed voxels. Moreover, these methods depend on the discretization of the space instead of the object itself which tends to be inefficient especially in cases where a significant part of the space grid is empty. A recent improvement on these methods suggests predicting only voxels on the surface to reduce the number of parameters and to opt for finer resolution [144].

Some researchers resorted to the multi-view representation where the depth information is implicit. Multi-view data are usually processed by parallel CNNs where each network processes a separate view and then the representations are all merged together for post-processing. Multi-view CNNs tend to perform better on recognition tasks in comparison with the volumetric data. This is more likely due to the various views of the 3D shape compared to one single volumetric view in the previous case. However, there are various trade-offs to such techniques. The sufficient number of views and the way they were acquired is a critical factor for representing the 3D shape. Also, the multi-view representation doesn't preserve the intrinsic geometric properties of the 3D shape. Experimental work as illustrated in table ?? shows a slightly higher accuracy of the multi-view methods in comparison to volumetric methods on recognition and classification tasks with less computations and parameters. However, a recent work managed to achieve the state-of-art recognition results on ModelNet dataset by using purely 3D volumetric model. However, this model is very complex in comparison to multi-view approaches and requires data augmentation as a crucial step in the pipeline. Moreover, the computational cost for processing such model is a bottleneck even with the existent powerful GPUs.

In conclusion, depending on the task and the available resources (data and hardware), one can decide on the suitable model to be used. Driven by the promising performance of both volumetric and multi-view CNNs, some efforts were directed towards fusing the advantages of both models which led to satisfying results [107]. Further investigations are now carried out to understand the drawbacks of these models and how to address them to speed up the training time.

4.3 Evolution of DL models on non-Euclidean 3D data representations

Recently, researchers started looking deeper into non-Euclidean 3D representations (point clouds, graphs and meshes) trying to define a new notion of convolution addressing the geometric challenges of such data. Most of the methods applied on point clouds can be roughly categorized into learning models and generating models. Learning models are concerned with learning the structure of point clouds for other tasks such as recognition and classification. In these models, the concept of neural networks is heavily used with the main purpose of learning the features of unordered point clouds. CNNs and RNNs are commonly used for learning the relationship between each point and

its neighborhood locally. However, these methods processed each point separately which is inconvenient for learning the global structure of the 3D point cloud. To overcome this shortcoming, some work proposed to use a recursive max pooling with clustering layer instead of the greedy winner-takes-all method. The second category, which is the generating models, are concerned with learning the intermediate features of the point clouds to be used for rendering and generating new data. Most of the techniques used for this purpose are unsupervised, variational AEs in specific and GANs. These methods allow for using much less training data without affecting the performance. Although some work has been done on analyzing point clouds, more efforts are directed towards analyzing graphs and meshes because such representations encode more information because of the availability of the surface information and connectivity between points, which is lacking in the point clouds representation.

A number of architectures that generalize the notion of convolution to graphs and meshes have been extensively studied lately suggesting two main directions: Spectral filtering and spatial filtering.

Spectral filtering depends on the eigen-decomposition of the graph-Laplacian to perform convolution on graphs in the spectral domain. However, these decompositions are often unstable and domain-dependent which makes the generalization across different shapes challenging. On the other hand, spatial filtering techniques rely on defining patches similar to the 2D signal in the Euclidean domain to perform the convolution on. These patches are either hard-coded on the graph or the mesh as illustrated in [16], [138], [139] or defined in terms of the topology of the 3D signal itself such as 1-hop neighborhood features as shown in [15]. These methods leverage the intrinsic geometric properties of the 3D shape and opens the door for a whole new research area. Although the undeniable innovations of these methods, they still suffer from some drawbacks.

Spatial networks where the patches are hand-crafted are computationally expensive due to the need to compute the defined patch on each vertex of the graph or the mesh. Beside that, some networks require extra processing on the convolutional filter itself to adapt to the extracted patches [138]. On the other hand, methods that exploit the topology information for patch definition reported better performance. It is important to note that these methods are local as all the processing is position dependent and not shift invariant. This can be seen in all the experiments reported in these papers, as non of these papers reported any results on recognition or retrieval tasks that require a global understanding of the 3D input data.

4.4 Future research directions

Recently, Elad et al. conducted extensive theoretical studies where they established a direct connection between CNNs and sparse coding in which they proved that the same properties of CNNs like locality, hierarchical feature maps and uniqueness of representation can be guaranteed with sparse modeling [145], [145], [146], [147]. The key idea of the proposed Convolutional Sparse Coding is to represent the whole signal in terms of one global dictionary that can

be decomposed into hierarchical dictionaries. This is defined in their work as Multi-Layer Convolutional Sparse Coding (ML-CSC). The learnt dictionaries in this framework are analogous to the feature maps in the CNN where they provide discriminative abstractions about the input data. This seems promising and opens the door for sparse modelling to act as a powerful learning model to uniquely represent the data similar to CNNs. However, the main drawback of this work is that it is purely theoretical and wasn't tested on real cases to see how it performs and how unique the learnt representations are. Moreover, This work has been initially started to analyze 1D and 2D signals like speech signals and images and is not yet extended to address 3D data. That is what pushed Quan et al. [148] to extend ML-CSC proposed by Elad to 3D data and test it on 3D voxels for feature learning and voxels classification in medical imaging tasks. Quan et al. proposed a new dictionary learning technique to operate on 3D voxels and decompose the learnt dictionary into multi-dictionaries for more abstraction. Experiments showed that this model is effective for the classification task where it was tested. However, it still suffers from serious limitations that might hold back the development of such field for 3D shape analysis. 3D ML-CSC was very expensive in terms of the computations needed (1.5GB of memory) to learn the dictionary and the max size of 3D data where it can be employed (365^3 voxels). These limitations act as a serious burden to apply the ML-CSC models on 3D data that is usually of much larger size than what these methods can handle and suffers from more problems such as noise and deformations, while these methods can only operate on synthetic or clean data as in [148].

The lack of the stability and practicality of the sparse modelling direction might limit its direct application on 3D data, however, it is an active area of research where new dictionary learning techniques are emerging and quickly developing.

ACKNOWLEDGMENTS

This work was supported by Artec 3D and the National Research Fund (FNR), Luxembourg, under the project IDform under the agreement C-PPP17/IS/11643091/IDform/Aouada.

REFERENCES

- [1] A. Krizhevsky, I. Sutskever, and G. E. Hinton, "Imagenet classification with deep convolutional neural networks," in *Advances in neural information processing systems*, 2012, pp. 1097–1105.
- [2] J. Long, E. Shelhamer, and T. Darrell, "Fully convolutional networks for semantic segmentation," in *Proceedings of the IEEE conference on computer vision and pattern recognition*, 2015, pp. 3431–3440.
- [3] H. Noh, S. Hong, and B. Han, "Learning deconvolution network for semantic segmentation," in *Proceedings of the IEEE International Conference on Computer Vision*, 2015, pp. 1520–1528.
- [4] S. Saito, T. Li, and H. Li, "Real-time facial segmentation and performance capture from rgb input," in *European Conference on Computer Vision*. Springer, 2016, pp. 244–261.
- [5] P. Sermanet, D. Eigen, X. Zhang, M. Mathieu, R. Fergus, and Y. LeCun, "Overfeat: Integrated recognition, localization and detection using convolutional networks," *arXiv preprint arXiv:1312.6229*, 2013.
- [6] K. He, X. Zhang, S. Ren, and J. Sun, "Deep residual learning for image recognition," in *Proceedings of the IEEE conference on computer vision and pattern recognition*, 2016, pp. 770–778.
- [7] C. Farabet, C. Couprie, L. Najman, and Y. LeCun, "Learning hierarchical features for scene labeling," *IEEE transactions on pattern analysis and machine intelligence*, vol. 35, no. 8, pp. 1915–1929, 2013.
- [8] J. Geng, "Structured-light 3d surface imaging: a tutorial," *Adv. Opt. Photon.*, vol. 3, no. 2, pp. 128–160, Jun 2011. [Online]. Available: <http://aop.osa.org/abstract.cfm?URI=aop-3-2-128>
- [9] M. Hansard, S. Lee, O. Choi, and R. Horaud, *Time-of-Flight Cameras: Principles, Methods and Applications*. Springer Publishing Company, Incorporated, 2012.
- [10] A. Sinha, J. Bai, and K. Ramani, "Deep learning 3d shape surfaces using geometry images," in *European Conference on Computer Vision*. Springer, 2016, pp. 223–240.
- [11] A. Brock, T. Lim, J. M. Ritchie, and N. Weston, "Generative and discriminative voxel modeling with convolutional neural networks," *arXiv preprint arXiv:1608.04236*, 2016.
- [12] D. Maturana and S. Scherer, "Voxnet: A 3d convolutional neural network for real-time object recognition," in *Intelligent Robots and Systems (IROS), 2015 IEEE/RSJ International Conference on*. IEEE, 2015, pp. 922–928.
- [13] Z. Wu, S. Song, A. Khosla, F. Yu, L. Zhang, X. Tang, and J. Xiao, "3d shapenets: A deep representation for volumetric shapes," in *Proceedings of the IEEE conference on computer vision and pattern recognition*, 2015, pp. 1912–1920.
- [14] N. Verma, E. Boyer, and J. Verbeek, "Feastnet: Feature-steered graph convolutions for 3d shape analysis," in *Proceedings of the IEEE Conference on Computer Vision and Pattern Recognition*, 2018, pp. 2598–2606.
- [15] M. Fey, J. E. Lenssen, F. Weichert, and H. Müller, "Splinecnn: Fast geometric deep learning with continuous b-spline kernels," *arXiv preprint arXiv:1711.08920*, 2017.
- [16] F. Monti, D. Boscaini, J. Masci, E. Rodola, J. Svoboda, and M. M. Bronstein, "Geometric deep learning on graphs and manifolds using mixture model cnns," in *Proc. CVPR*, vol. 1, no. 2, 2017, p. 3.
- [17] H. Maron, M. Galun, N. Aigerman, M. Trope, N. Dym, E. Yumer, V. G. Kim, and Y. Lipman, "Convolutional neural networks on surfaces via seamless toric covers," *ACM Trans. Graph*, vol. 36, no. 4, p. 71, 2017.
- [18] M. M. Bronstein, J. Bruna, Y. LeCun, A. Szlam, and P. Vandergheynst, "Geometric deep learning: going beyond euclidean data," *IEEE Signal Processing Magazine*, vol. 34, no. 4, pp. 18–42, 2017.
- [19] A. Ioannidou, E. Chatzilari, S. Nikolopoulos, and I. Kompatsiaris, "Deep learning advances in computer vision with 3d data: A survey," *ACM Computing Surveys (CSUR)*, vol. 50, no. 2, p. 20, 2017.
- [20] A. Bronstein and M. Bronstein, 2007. [Online]. Available: <http://vision.mas.ecp.fr/Personnel/iasonas/descriptors.html>
- [21] K. Lai, L. Bo, X. Ren, and D. Fox, "A large-scale hierarchical multi-view rgb-d object dataset," in *Robotics and Automation (ICRA), 2011 IEEE International Conference on*. IEEE, 2011, pp. 1817–1824.
- [22] S. H. Sylvain Lefebvre and F. Neyret, April, 2005. [Online]. Available: <https://developer.nvidia.com/gpugems/GPUGems2.html>
- [23] H. Su, S. Maji, E. Kalogerakis, and E. Learned-Miller, "Multi-view convolutional neural networks for 3d shape recognition," in *Proceedings of the IEEE international conference on computer vision*, 2015, pp. 945–953.
- [24] A. Bronstein and M. Bronstein, "Discrete geometry tutorial 1," May 2018.
- [25] K. Berger, "The role of rgb-d benchmark datasets: an overview," *arXiv preprint arXiv:1310.2053*, 2013.
- [26] Y. Guo, J. Zhang, M. Lu, J. Wan, and Y. Ma, "Benchmark datasets for 3d computer vision," in *Industrial Electronics and Applications (ICIEA), 2014 IEEE 9th Conference on*. IEEE, 2014, pp. 1846–1851.
- [27] C. Chen, R. Jafari, and N. Kehtarnavaz, "Utd-mhad: A multi-modal dataset for human action recognition utilizing a depth camera and a wearable inertial sensor," in *Image Processing (ICIP), 2015 IEEE International Conference on*. IEEE, 2015, pp. 168–172.
- [28] M. Firman, "RGBD Datasets: Past, Present and Future," in *CVPR Workshop on Large Scale 3D Data: Acquisition, Modelling and Analysis*, 2016.
- [29] I. K. Kazmi, L. You, and J. J. Zhang, "A survey of 2d and 3d shape descriptors," in *Computer graphics, imaging and visualization (cgiv), 2013 10th international conference*. IEEE, 2013, pp. 1–10.

- [30] L. Zhang, M. J. da Fonseca, A. Ferreira, and C. R. A. e Recuperação, "Survey on 3d shape descriptors," *Fundação para a Ciência e Tecnologia, Lisboa, Portugal, Tech. Rep. Technical Report, DecorAR (FCT POSC/EIA/59938/2004)*, vol. 3, 2007.
- [31] W. Wohlkinger and M. Vincze, "Ensemble of shape functions for 3d object classification," in *Robotics and Biomimetics (ROBIO), 2011 IEEE International Conference on*. IEEE, 2011, pp. 2987–2992.
- [32] A. Aldoma, F. Tombari, R. B. Rusu, and M. Vincze, "Our-cvfh-oriented, unique and repeatable clustered viewpoint feature histogram for object recognition and 6dof pose estimation," in *Joint DAGM (German Association for Pattern Recognition) and OAGM Symposium*. Springer, 2012, pp. 113–122.
- [33] Z.-C. Marton, D. Pangercic, N. Blodow, and M. Beetz, "Combined 2d–3d categorization and classification for multimodal perception systems," *The International Journal of Robotics Research*, vol. 30, no. 11, pp. 1378–1402, 2011.
- [34] R. B. Rusu, N. Blodow, and M. Beetz, "Fast point feature histograms (fpfh) for 3d registration," in *Robotics and Automation, 2009. ICRA'09. IEEE International Conference on*. IEEE, 2009, pp. 3212–3217.
- [35] L. Yi, V. G. Kim, D. Ceylan, I. Shen, M. Yan, H. Su, C. Lu, Q. Huang, A. Sheffer, L. Guibas *et al.*, "A scalable active framework for region annotation in 3d shape collections," *ACM Transactions on Graphics (TOG)*, vol. 35, no. 6, p. 210, 2016.
- [36] A. E. Johnson and M. Hebert, "Using spin images for efficient object recognition in cluttered 3d scenes," *IEEE Transactions on pattern analysis and machine intelligence*, vol. 21, no. 5, pp. 433–449, 1999.
- [37] Y. Guo, F. Sohel, M. Bennamoun, M. Lu, and J. Wan, "Rotational projection statistics for 3d local surface description and object recognition," *International journal of computer vision*, vol. 105, no. 1, pp. 63–86, 2013.
- [38] M. M. Bronstein and I. Kokkinos, "Scale-invariant heat kernel signatures for non-rigid shape recognition," in *Computer Vision and Pattern Recognition (CVPR), 2010 IEEE Conference on*. IEEE, 2010, pp. 1704–1711.
- [39] M. Aubry, U. Schlickewei, and D. Cremers, "The wave kernel signature: A quantum mechanical approach to shape analysis," in *Computer Vision Workshops (ICCV Workshops), 2011 IEEE International Conference on*. IEEE, 2011, pp. 1626–1633.
- [40] D. Aouada, S. Feng, and H. Krim, "Statistical analysis of the global geodesic function for 3d object classification," in *2007 IEEE International Conference on Acoustics, Speech and Signal Processing - ICASSP '07*, vol. 1, April 2007, pp. 1–645–1–648.
- [41] D. Aouada, D. W. Dreisigmeyer, and H. Krim, "Geometric modeling of rigid and non-rigid 3d shapes using the global geodesic function," in *2008 IEEE Computer Society Conference on Computer Vision and Pattern Recognition Workshops*, June 2008, pp. 1–8.
- [42] D. Aouada and H. Krim, "Squigraphs for fine and compact modeling of 3-d shapes," *IEEE Transactions on Image Processing*, vol. 19, no. 2, pp. 306–321, Feb 2010.
- [43] J. Sun, M. Ovsjanikov, and L. Guibas, "A concise and provably informative multi-scale signature based on heat diffusion," in *Computer graphics forum*, vol. 28, no. 5. Wiley Online Library, 2009, pp. 1383–1392.
- [44] D.-Y. Chen, X.-P. Tian, Y.-T. Shen, and M. Ouhyoung, "On visual similarity based 3d model retrieval," in *Computer graphics forum*, vol. 22, no. 3. Wiley Online Library, 2003, pp. 223–232.
- [45] H. Ling and D. W. Jacobs, "Shape classification using the inner-distance," *IEEE transactions on pattern analysis and machine intelligence*, vol. 29, no. 2, pp. 286–299, 2007.
- [46] R. B. Rusu, N. Blodow, Z. C. Marton, and M. Beetz, "Aligning point cloud views using persistent feature histograms," in *Intelligent Robots and Systems, 2008. IROS 2008. IEEE/RSJ International Conference on*. IEEE, 2008, pp. 3384–3391.
- [47] Z. Cao, Q. Huang, and K. Ramani, "3d object classification via spherical projections," *arXiv preprint arXiv:1712.04426*, 2017.
- [48] B. Shi, S. Bai, Z. Zhou, and X. Bai, "Deeppano: Deep panoramic representation for 3-d shape recognition," *IEEE Signal Processing Letters*, vol. 22, no. 12, pp. 2339–2343, 2015.
- [49] J. Han, L. Shao, D. Xu, and J. Shotton, "Enhanced computer vision with microsoft kinect sensor: A review," *IEEE transactions on cybernetics*, vol. 43, no. 5, pp. 1318–1334, 2013.
- [50] N. Erdogmus and S. Marcel, "Spoofing in 2d face recognition with 3d masks and anti-spoofing with kinect," in *Biometrics: Theory, Applications and Systems (BTAS), 2013 IEEE Sixth International Conference on*. IEEE, 2013, pp. 1–6.
- [51] G. Fanelli, T. Weise, J. Gall, and L. Van Gool, "Real time head pose estimation from consumer depth cameras," in *Joint Pattern Recognition Symposium*. Springer, 2011, pp. 101–110.
- [52] M. Zollhöfer, M. Nießner, S. Izadi, C. Rehmann, C. Zach, M. Fisher, C. Wu, A. Fitzgibbon, C. Loop, C. Theobalt *et al.*, "Real-time non-rigid reconstruction using an rgb-d camera," *ACM Transactions on Graphics (TOG)*, vol. 33, no. 4, p. 156, 2014.
- [53] Y. Xiang, W. Choi, Y. Lin, and S. Savarese, "Data-driven 3d voxel patterns for object category recognition," in *Proceedings of the IEEE Conference on Computer Vision and Pattern Recognition*, 2015, pp. 1903–1911.
- [54] A. Abdul-Rahman and M. Pilouk, *Spatial data modelling for 3D GIS*. Springer Science & Business Media, 2007.
- [55] M. Tatarchenko, A. Dosovitskiy, and T. Brox, "Octree generating networks: Efficient convolutional architectures for high-resolution 3d outputs," *CoRR, abs/1703.09438*, 2017.
- [56] F. Dong, "Three-dimensional models and applications in subsurface modeling," 1996.
- [57] H. Samet, "The quadtree and related hierarchical data structures," *ACM Computing Surveys (CSUR)*, vol. 16, no. 2, pp. 187–260, 1984.
- [58] J. Zhao, X. Xie, X. Xu, and S. Sun, "Multi-view learning overview: Recent progress and new challenges," *Information Fusion*, vol. 38, pp. 43–54, 2017.
- [59] L. Yin, X. Wei, Y. Sun, J. Wang, and M. J. Rosato, "A 3d facial expression database for facial behavior research," in *Automatic face and gesture recognition, 2006. FGR 2006. 7th international conference on*. IEEE, 2006, pp. 211–216.
- [60] B.-Q. Shi, J. Liang, and Q. Liu, "Adaptive simplification of point cloud using k-means clustering," *Computer-Aided Design*, vol. 43, no. 8, pp. 910–922, 2011.
- [61] B. Huhle, T. Schairer, P. Jenke, and W. Straßer, "Robust non-local denoising of colored depth data," in *Computer Vision and Pattern Recognition Workshops, 2008. CVPRW'08. IEEE Computer Society Conference on*. IEEE, 2008, pp. 1–7.
- [62] P. Jenke, M. Wand, M. Bokeloh, A. Schilling, and W. Straßer, "Bayesian point cloud reconstruction," in *Computer Graphics Forum*, vol. 25, no. 3. Wiley Online Library, 2006, pp. 379–388.
- [63] J. Park, H. Kim, Y.-W. Tai, M. S. Brown, and I. Kweon, "High quality depth map upsampling for 3d-tof cameras," in *Computer Vision (ICCV), 2011 IEEE International Conference on*. IEEE, 2011, pp. 1623–1630.
- [64] J. C. Rangel, V. Morell, M. Cazorla, S. Orts-Escolano, and J. Garcia-Rodríguez, "Object recognition in noisy rgb-d data using gng," *Pattern Analysis and Applications*, vol. 20, no. 4, pp. 1061–1076, 2017.
- [65] C. Yan, H. Xie, D. Yang, J. Yin, Y. Zhang, and Q. Dai, "Supervised hash coding with deep neural network for environment perception of intelligent vehicles," *IEEE transactions on intelligent transportation systems*, vol. 19, no. 1, pp. 284–295, 2018.
- [66] X.-F. Han, J. S. Jin, M.-J. Wang, and W. Jiang, "Guided 3d point cloud filtering," *Multimedia Tools and Applications*, pp. 1–15, 2017.
- [67] L. Cosmo, E. Rodolà, M. Bronstein, A. Torsello, D. Cremers, and Y. Sahillioglu, "Shrec'16: Partial matching of deformable shapes," *Proc. 3DOR*, vol. 2, no. 9, p. 12, 2016.
- [68] J. W. Tangelder and R. C. Veltkamp, "A survey of content based 3d shape retrieval methods," in *Shape Modeling Applications, 2004. Proceedings.* IEEE, 2004, pp. 145–156.
- [69] Z.-B. Liu, S.-H. Bu, K. Zhou, S.-M. Gao, J.-W. Han, and J. Wu, "A survey on partial retrieval of 3d shapes," *Journal of Computer Science and Technology*, vol. 28, no. 5, pp. 836–851, 2013.
- [70] Z. Liu, S. Chen, S. Bu, and K. Li, "High-level semantic feature for 3d shape based on deep belief networks," in *Multimedia and Expo (ICME), 2014 IEEE International Conference on*. IEEE, 2014, pp. 1–6.
- [71] S. Bu, Z. Liu, J. Han, J. Wu, and R. Ji, "Learning high-level feature by deep belief networks for 3-d model retrieval and recognition," *IEEE Transactions on Multimedia*, vol. 16, pp. 2154–2167, 2014.
- [72] S. Bu, P. Han, Z. Liu, J. Han, and H. Lin, "Local deep feature learning framework for 3d shape," *Computers & Graphics*, vol. 46, pp. 117–129, 2015.
- [73] Z. Xie, K. Xu, W. Shan, L. Liu, Y. Xiong, and H. Huang, "Projective feature learning for 3d shapes with multi-view depth images," in *Computer Graphics Forum*, vol. 34, no. 7. Wiley Online Library, 2015, pp. 1–11.
- [74] Z. Han, Z. Liu, J. Han, C.-M. Vong, S. Bu, and C. L. P. Chen, "Mesh convolutional restricted boltzmann machines for unsupervised

- learning of features with structure preservation on 3-d meshes," *IEEE transactions on neural networks and learning systems*, vol. 28, no. 10, pp. 2268–2281, 2017.
- [75] Z. Zhu, X. Wang, S. Bai, C. Yao, and X. Bai, "Deep learning representation using autoencoder for 3d shape retrieval," *Neurocomputing*, vol. 204, pp. 41–50, 2016.
- [76] K. Sfikas, T. Theoharis, and I. Pratikakis, "Exploiting the panorama representation for convolutional neural network classification and retrieval," in *Eurographics Workshop on 3D Object Retrieval*, 2017.
- [77] K. Sfikas, I. Pratikakis, and T. Theoharis, "Ensemble of panorama-based convolutional neural networks for 3d model classification and retrieval," *Computers & Graphics*, 2017.
- [78] R. Socher, B. Huval, B. Bath, C. D. Manning, and A. Y. Ng, "Convolutional-recursive deep learning for 3d object classification," in *Advances in Neural Information Processing Systems*, 2012, pp. 656–664.
- [79] C. Couprie, C. Farabet, L. Najman, and Y. LeCun, "Indoor semantic segmentation using depth information," *arXiv preprint arXiv:1301.3572*, 2013.
- [80] A. Eitel, J. T. Springenberg, L. Spinello, M. Riedmiller, and W. Burgard, "Multimodal deep learning for robust rgb-d object recognition," in *Intelligent Robots and Systems (IROS), 2015 IEEE/RSJ International Conference on*. IEEE, 2015, pp. 681–687.
- [81] J. Feng, Y. Wang, and S.-F. Chang, "3d shape retrieval using a single depth image from low-cost sensors," in *Applications of Computer Vision (WACV), 2016 IEEE Winter Conference on*. IEEE, 2016, pp. 1–9.
- [82] L. A. Alexandre, "3d object recognition using convolutional neural networks with transfer learning between input channels," in *Intelligent Autonomous Systems 13*. Springer, 2016, pp. 889–898.
- [83] M. Schwarz, H. Schulz, and S. Behnke, "Rgb-d object recognition and pose estimation based on pre-trained convolutional neural network features," in *Robotics and Automation (ICRA), 2015 IEEE International Conference on*. IEEE, 2015, pp. 1329–1335.
- [84] H. Lee, R. Grosse, R. Ranganath, and A. Y. Ng, "Convolutional deep belief networks for scalable unsupervised learning of hierarchical representations," in *Proceedings of the 26th annual international conference on machine learning*. ACM, 2009, pp. 609–616.
- [85] N. Sedaghat, M. Zolfaghari, E. Amiri, and T. Brox, "Orientation-boosted voxel nets for 3d object recognition," *arXiv preprint arXiv:1604.03351*, 2016.
- [86] J. Wu, C. Zhang, T. Xue, B. Freeman, and J. Tenenbaum, "Learning a probabilistic latent space of object shapes via 3d generative-adversarial modeling," in *Advances in Neural Information Processing Systems*, 2016, pp. 82–90.
- [87] C. Szegedy, S. Ioffe, V. Vanhoucke, and A. A. Alemi, "Inception-v4, inception-resnet and the impact of residual connections on learning," in *AAAI*, vol. 4, 2017, p. 12.
- [88] S. Ioffe and C. Szegedy, "Batch normalization: Accelerating deep network training by reducing internal covariate shift," *arXiv preprint arXiv:1502.03167*, 2015.
- [89] G. Huang, Y. Sun, Z. Liu, D. Sedra, and K. Q. Weinberger, "Deep networks with stochastic depth," in *European Conference on Computer Vision*. Springer, 2016, pp. 646–661.
- [90] X. Xu and S. Todorovic, "Beam search for learning a deep convolutional neural network of 3d shapes," in *Pattern Recognition (ICPR), 2016 23rd International Conference on*. IEEE, 2016, pp. 3506–3511.
- [91] S. Song and J. Xiao, "Deep Sliding Shapes for amodal 3D object detection in RGB-D images," 2016.
- [92] S. Zhi, Y. Liu, X. Li, and Y. Guo, "Toward real-time 3d object recognition: A lightweight volumetric cnn framework using multitask learning," *Computers & Graphics*, 2017.
- [93] B. Leng, X. Zhang, M. Yao, and Z. Xiong, "3d object classification using deep belief networks," in *International Conference on Multimedia Modeling*. Springer, 2014, pp. 128–139.
- [94] P. Daras and A. Axenopoulos, "A 3d shape retrieval framework supporting multimodal queries," *International Journal of Computer Vision*, vol. 89, no. 2-3, pp. 229–247, 2010.
- [95] B. Leng, S. Guo, X. Zhang, and Z. Xiong, "3d object retrieval with stacked local convolutional autoencoder," *Signal Processing*, vol. 112, pp. 119–128, 2015.
- [96] B. Leng, Y. Liu, K. Yu, X. Zhang, and Z. Xiong, "3d object understanding with 3d convolutional neural networks," *Information sciences*, vol. 366, pp. 188–201, 2015.
- [97] E. Johns, S. Leutenegger, and A. J. Davison, "Pairwise decomposition of image sequences for active multi-view recognition," in *Computer Vision and Pattern Recognition (CVPR), 2016 IEEE Conference on*. IEEE, 2016, pp. 3813–3822.
- [98] S. Bai, X. Bai, Z. Zhou, Z. Zhang, and L. J. Latecki, "Gift: A real-time and scalable 3d shape search engine," in *Computer Vision and Pattern Recognition (CVPR), 2016 IEEE Conference on*. IEEE, 2016, pp. 5023–5032.
- [99] P. Zanuttigh and L. Minto, "Deep learning for 3d shape classification from multiple depth maps," in *Proceedings of IEEE International Conference on Image Processing (ICIP)*, 2017.
- [100] C. Wang, M. Pelillo, and K. Siddiqi, "Dominant set clustering and pooling for multi-view 3d object recognition," in *Proceedings of British Machine Vision Conference (BMVC)*, 2017.
- [101] C. R. Qi, H. Su, M. Nießner, A. Dai, M. Yan, and L. J. Guibas, "Volumetric and multi-view cnns for object classification on 3d data," in *Proceedings of the IEEE conference on computer vision and pattern recognition*, 2016, pp. 5648–5656.
- [102] F. Wang, L. Kang, and Y. Li, "Sketch-based 3d shape retrieval using convolutional neural networks," in *Computer Vision and Pattern Recognition (CVPR), 2015 IEEE Conference on*. IEEE, 2015, pp. 1875–1883.
- [103] Y. Wang, Z. Xie, K. Xu, Y. Dou, and Y. Lei, "An efficient and effective convolutional auto-encoder extreme learning machine network for 3d feature learning," *Neurocomputing*, vol. 174, pp. 988–998, 2016.
- [104] G.-B. Huang, Q.-Y. Zhu, and C.-K. Siew, "Extreme learning machine: theory and applications," *Neurocomputing*, vol. 70, no. 1-3, pp. 489–501, 2006.
- [105] L. L. C. Kasun, H. Zhou, G.-B. Huang, and C. M. Vong, "Representational learning with elms for big data," 2013.
- [106] Y. Ben-Shabat, M. Lindenbaum, and A. Fischer, "3d point cloud classification and segmentation using 3d modified fisher vector representation for convolutional neural networks," *arXiv preprint arXiv:1711.08241*, 2017.
- [107] V. Hegde and R. Zadeh, "Fusionnet: 3d object classification using multiple data representations," *arXiv preprint arXiv:1607.05695*, 2016.
- [108] O. Vinyals, S. Bengio, and M. Kudlur, "Order matters: Sequence to sequence for sets," *arXiv preprint arXiv:1511.06391*, 2015.
- [109] S. Ravanbakhsh, J. Schneider, and B. Póczos, "Deep learning with sets and point clouds," *arXiv preprint arXiv:1611.04500*, 2016.
- [110] M. Zaheer, S. Kottur, S. Ravanbakhsh, B. Póczos, R. R. Salakhutdinov, and A. J. Smola, "Deep sets," in *Advances in Neural Information Processing Systems*, 2017, pp. 3394–3404.
- [111] C. R. Qi, H. Su, K. Mo, and L. J. Guibas, "Pointnet: Deep learning on point sets for 3d classification and segmentation," *arXiv preprint arXiv:1612.00593*, 2016.
- [112] —, "Pointnet: Deep learning on point sets for 3d classification and segmentation," *Proc. Computer Vision and Pattern Recognition (CVPR), IEEE*, vol. 1, no. 2, p. 4, 2017.
- [113] C. R. Qi, L. Yi, H. Su, and L. J. Guibas, "Pointnet++: Deep hierarchical feature learning on point sets in a metric space," in *Advances in Neural Information Processing Systems*, 2017, pp. 5105–5114.
- [114] R. Kulkov and V. Lempitsky, "Escape from cells: Deep kd-networks for the recognition of 3d point cloud models," in *2017 IEEE International Conference on Computer Vision (ICCV)*. IEEE, 2017, pp. 863–872.
- [115] R. Roveri, L. Rahmann, A. C. Oztireli, and M. Gross, "A network architecture for point cloud classification via automatic depth images generation," in *Proceedings of the IEEE Conference on Computer Vision and Pattern Recognition*, 2018, pp. 4176–4184.
- [116] K. He, X. Zhang, S. Ren, and J. Sun, "Deep residual learning for image recognition," *arXiv preprint arXiv:1512.03385*, 2015.
- [117] Y. Yang, C. Feng, Y. Shen, and D. Tian, "Foldingnet: Point cloud auto-encoder via deep grid deformation," in *Proc. IEEE Conf. on Computer Vision and Pattern Recognition (CVPR)*, vol. 3, 2018.
- [118] J. Li, B. M. Chen, and G. H. Lee, "So-net: Self-organizing network for point cloud analysis," *arXiv preprint arXiv:1803.04249*, 2018.
- [119] J. Bruna, W. Zaremba, A. Szlam, and Y. LeCun, "Spectral networks and locally connected networks on graphs," *arXiv preprint arXiv:1312.6203*, 2013.
- [120] A. Kovnatsky, M. M. Bronstein, A. M. Bronstein, K. Glashoff, and R. Kimmel, "Coupled quasi-harmonic bases," in *Computer Graphics Forum*, vol. 32, no. 2pt4. Wiley Online Library, 2013, pp. 439–448.

- [121] M. Defferrard, X. Bresson, and P. Vandergheynst, "Convolutional neural networks on graphs with fast localized spectral filtering," in *Advances in Neural Information Processing Systems*, 2016, pp. 3844–3852.
- [122] T. N. Kipf and M. Welling, "Semi-supervised classification with graph convolutional networks," *arXiv preprint arXiv:1609.02907*, 2016.
- [123] C. Wang, B. Samari, and K. Siddiqi, "Local spectral graph convolution for point set feature learning," *arXiv preprint arXiv:1803.05827*, 2018.
- [124] F. Scarselli, M. Gori, A. C. Tsoi, M. Hagenbuchner, and G. Monfardini, "The graph neural network model," *IEEE Transactions on Neural Networks*, vol. 20, no. 1, pp. 61–80, 2009.
- [125] Y. Li, D. Tarlow, M. Brockschmidt, and R. Zemel, "Gated graph sequence neural networks," *arXiv preprint arXiv:1511.05493*, 2015.
- [126] S. Sukhbaatar, R. Fergus *et al.*, "Learning multiagent communication with backpropagation," in *Advances in Neural Information Processing Systems*, 2016, pp. 2244–2252.
- [127] D. K. Duvenaud, D. Maclaurin, J. Iparraguirre, R. Bombarell, T. Hirzel, A. Aspuru-Guzik, and R. P. Adams, "Convolutional networks on graphs for learning molecular fingerprints," in *Advances in neural information processing systems*, 2015, pp. 2224–2232.
- [128] M. B. Chang, T. Ullman, A. Torralba, and J. B. Tenenbaum, "A compositional object-based approach to learning physical dynamics," *arXiv preprint arXiv:1612.00341*, 2016.
- [129] P. Battaglia, R. Pascanu, M. Lai, D. J. Rezende *et al.*, "Interaction networks for learning about objects, relations and physics," in *Advances in neural information processing systems*, 2016, pp. 4502–4510.
- [130] M. Gori, G. Monfardini, and F. Scarselli, "A new model for learning in graph domains," in *Neural Networks, 2005. IJCNN'05. Proceedings. 2005 IEEE International Joint Conference on*, vol. 2. IEEE, 2005, pp. 729–734.
- [131] A. Coates and A. Y. Ng, "Selecting receptive fields in deep networks," in *Advances in Neural Information Processing Systems*, 2011, pp. 2528–2536.
- [132] K. Gregor and Y. LeCun, "Emergence of complex-like cells in a temporal product network with local receptive fields," *arXiv preprint arXiv:1006.0448*, 2010.
- [133] M. Niepert, M. Ahmed, and K. Kutzkov, "Learning convolutional neural networks for graphs," in *International conference on machine learning*, 2016, pp. 2014–2023.
- [134] S. B. Venkatakrisnan, M. Alizadeh, and P. Viswanath, "Graph2seq: Scalable learning dynamics for graphs," *arXiv preprint arXiv:1802.04948*, 2018.
- [135] E. Khalil, H. Dai, Y. Zhang, B. Dilkina, and L. Song, "Learning combinatorial optimization algorithms over graphs," in *Advances in Neural Information Processing Systems*, 2017, pp. 6351–6361.
- [136] A. Nowak, S. Villar, A. S. Bandeira, and J. Bruna, "A note on learning algorithms for quadratic assignment with graph neural networks," *arXiv preprint arXiv:1706.07450*, 2017.
- [137] J. Bruna and X. Li, "Community detection with graph neural networks," *arXiv preprint arXiv:1705.08415*, 2017.
- [138] J. Masci, D. Boscaini, M. Bronstein, and P. Vandergheynst, "Geodesic convolutional neural networks on riemannian manifolds," in *Proceedings of the IEEE international conference on computer vision workshops*, 2015, pp. 37–45.
- [139] D. Boscaini, J. Masci, E. Rodolà, and M. Bronstein, "Learning shape correspondence with anisotropic convolutional neural networks," in *Advances in Neural Information Processing Systems*, 2016, pp. 3189–3197.
- [140] J. Deng, W. Dong, R. Socher, L.-J. Li, K. Li, and L. Fei-Fei, "ImageNet: A Large-Scale Hierarchical Image Database," in *CVPR09*, 2009.
- [141] S. Song, F. Yu, A. Zeng, A. X. Chang, M. Savva, and T. Funkhouser, "Semantic scene completion from a single depth image," in *Computer Vision and Pattern Recognition (CVPR), 2017 IEEE Conference on*. IEEE, 2017, pp. 190–198.
- [142] A. Handa, V. Pătrăucean, S. Stent, and R. Cipolla, "Scenenet: An annotated model generator for indoor scene understanding," in *Robotics and Automation (ICRA), 2016 IEEE International Conference on*. IEEE, 2016, pp. 5737–5743.
- [143] A. Dai, A. X. Chang, M. Savva, M. Halber, T. Funkhouser, and M. Nießner, "Scannet: Richly-annotated 3d reconstructions of indoor scenes," in *Proc. IEEE Conf. on Computer Vision and Pattern Recognition (CVPR)*, vol. 1, 2017.
- [144] C. Häne, S. Tulsiani, and J. Malik, "Hierarchical surface prediction for 3d object reconstruction," *arXiv preprint arXiv:1704.00710*, 2017.
- [145] V. Pappayan, Y. Romano, and M. Elad, "Convolutional neural networks analyzed via convolutional sparse coding," *stat*, vol. 1050, p. 27, 2016.
- [146] J. Sulam, V. Pappayan, Y. Romano, and M. Elad, "Multi-layer convolutional sparse modeling: Pursuit and dictionary learning," *arXiv preprint arXiv:1708.08705*, 2017.
- [147] M. Elad *et al.*, "Sparse modeling in image processing and deep learning (keynote talk)," 2018.
- [148] T. M. Quan, J. Choi, H. Jeong, and W.-K. Jeong, "An intelligent system approach for probabilistic volume rendering using hierarchical 3d convolutional sparse coding," *IEEE transactions on visualization and computer graphics*, vol. 24, no. 1, pp. 964–973, 2018.